

Mars as an Exoplanet: Lessons from a Planet at the Edge of Habitability

STEPHEN R. KANE,¹ PAUL K. BYRNE,² SKYLAR D'ANGIOLILLO,¹ MICHELLE L. HILL,^{1,3} EMMA L. MILES,¹
DAVID A. BRAIN,⁴ SHANNON M. CURRY,⁴ AND JOANA R.C. VOIGT¹

¹*Department of Earth and Planetary Sciences, University of California, Riverside, CA 92521, USA*

²*Department of Earth, Environmental, and Planetary Sciences, Washington University, St. Louis, MO 63130, USA*

³*Department of Earth and Planetary Sciences, Stanford University, Stanford, CA 94305, USA*

⁴*Laboratory for Atmospheric and Space Physics, University of Colorado, Boulder, CO 80304, USA*

ABSTRACT

Mars is the Solar System's canonical small, rocky planet that transitioned from early geologic activity and surface liquid water to a cold and arid planet with a thin, cold, CO₂-dominated atmosphere. The evolution of Mars, in the context of such planetary parameters as size, mass, atmosphere, insolation flux, magnetosphere, and impact history, harbor important diagnostics regarding the development and sustainability of habitable surface conditions. In this work, we synthesize how the study of Mars contributes to our understanding of exoplanet processes, such as volatile delivery and loss, photochemistry, climate evolution (including CO₂ condensation and atmospheric loss), obliquity forcing, planetary architecture, and the role of intrinsic magnetism. We also evaluate optimal methods and prospects for detecting and characterizing potential Mars analogs beyond the Solar System. We focus on relevant results from planetary missions (e.g., Mars Reconnaissance Orbiter, MAVEN, Mars Science Laboratory, Mars2020) and observational studies of exoplanet atmospheres with the James Webb Space telescope (JWST) and future facilities. Through the convergence of these parallel pathways of inquiry, we describe the primary science questions and suggested avenues for characterizing small rocky planets that lie at the edge of potentially habitable conditions.

Keywords: astrobiology – planetary systems – planets and satellites: individual (Mars)

1. INTRODUCTION

Exoplanet discoveries have advanced tremendously over the past few decades, including the exploration of the demographics into the terrestrial regime (Ford 2014; Winn & Fabrycky 2015; Christiansen et al. 2025), and even those worlds that lie within their system's Habitable Zone (HZ) (Kasting et al. 1993; Kane & Gelino 2012a; Kopparapu et al. 2013, 2014; Kane et al. 2016; Hill et al. 2018, 2023). Results from exoplanet surveys have demonstrated that small planets are more common than their giant planetary cousins (Howard et al. 2010; Dressing & Charbonneau 2015), creating an interesting comparison to the Solar System's architecture (Martin & Livio 2015; Horner et al. 2020; Raymond et al. 2020; Kane et al. 2021b). Yet, despite their relatively high occurrence, the climates, volatile budgets,

and long-term habitability of small terrestrial planets remain poorly understood (Tasker et al. 2017; Adams et al. 2025; Apai et al. 2025). Venus, Earth, Mars, and even the Moon each underwent distinct volatile, tectonic, and atmospheric trajectories despite sharing the same stellar environment, illustrating that planet size alone does not uniquely determine planetary evolution (Jakosky & Byrne 2025; Kane et al. 2021b). A complete framework for interpreting rocky exoplanets will ultimately require integrating lessons from all of these bodies. With that broader context in mind, we focus here on Mars because its sub-Earth mass, thin atmosphere, and rich in-situ dataset make it particularly instructive for the low-mass, volatile-poor regime that many detected rocky exoplanets may inhabit. In that sense, Mars offers a uniquely data-rich end-member: a sub-Earth-mass planet ($0.107 M_{\oplus}$, $0.53 R_{\oplus}$) that lost most of its atmosphere and surface water early, leaving isotopic fingerprints in the residual gases and surface record (Hu et al. 2015; Jakosky et al. 2017; Jakosky 2021). Mars

thus grounds our models of escape physics, volatile cycling without plate tectonics, and climate feedbacks that can drive atmospheres toward collapse—phenomena anticipated on many close-in M-dwarf planets.

Mars occupies a singular position in comparative planetary geology: it is simultaneously a well-observed planetary neighbor with a rich rock and climate record, and a physical regime (low gravity, thin atmosphere, volatile sensitivity) that is highly relevant to the smallest rocky exoplanets we are currently able to detect. Orbital spectroscopy and in situ exploration reveal a basaltic crust variably altered by water, with widespread phyllosilicates and sulfates that encode a transition from early, more clement conditions to later aridity (Ehlmann & Edwards 2014). Stratigraphic and geochemical observations at Gale crater demonstrate sustained lacustrine deposition with redox gradients, pointing to environments that were habitable (and chemically diverse) for geologically significant intervals (Hurowitz et al. 2017). At the same time, Mars demonstrates how small planetary size and gravity shape climate evolution. Crustal magnetization patterns measured by Mars Global Surveyor imply an early, now-extinct global dynamo (Acuna et al. 1999; Connerney et al. 1999), with isotopic signatures such as $^{40}\text{Ar}/^{36}\text{Ar}$ and D/H evidencing extensive atmospheric escape thereafter. The Mars Atmosphere and Volatile Evolution (MAVEN) mission quantified present-day loss channels (H, O, and ions) and, by integrating over enhanced early solar activity, showed that escape plausibly removed a large fraction of an early, thicker atmosphere (Jakosky et al. 2018). Together, the geology and atmospheric evolution record of Mars offers a deeper understanding of fundamental processes that are directly transferable to interpreting surface-interior-atmosphere coupling on small exoplanets (Shoji & Kurita 2014; Khuller & Clow 2024; Jakosky & Byrne 2025).

Furthermore, Mars’ climate physics maps naturally onto exoplanet modeling regimes of interest. Its $\text{CO}_2\text{--H}_2\text{O}$ photochemistry and HO_x -controlled oxidant budgets connect to generalized small-planet photochemistry (Lefèvre & Forget 2009); chaotic obliquity cycles and dust–radiation feedbacks offer a template for forcings that may episodically reshape sub-Earth climates (Ward 1973; Touma & Wisdom 1993; Jakosky et al. 1995; Forget et al. 2006; Kane et al. 2025); and its transition from wetter Noachian–Hesperian to cold–dry Amazonian environments provides boundary conditions for testing long-term habitability on small worlds (Nair et al. 1994; Zahnle et al. 2008). Mars is also an important case-study in terrestrial atmospheric retention; an aspect that has greatly shaped the early habitable

history of the planet and has great relevance to similarly sized exoplanets (Jakosky et al. 1994; Chassefière & Leblanc 2004; Tian et al. 2009; Lammer et al. 2013; Dong et al. 2018b; Basak & Nandy 2021). The atmospheric loss processes that have and continue to occur at Mars thus inform the development of models that may be applied to a variety of exoplanet contexts (Lammer et al. 2008; Owen 2019). These models are particularly applicable to the TRAPPIST-1 system (Roettenbacher & Kane 2017; Dong et al. 2018a), whose relatively small size, proximity to the host star, and age, may have resulted in their atmospheric desiccation (Greene et al. 2023; Zieba et al. 2023; Piaulet-Ghorayeb et al. 2025), underscoring the potential atmospheric vulnerability around active M-dwarfs. These planetary properties, anchored by laboratory, orbital, and surface measurements, make Mars an indispensable analog for connecting process-level planetary science to the maturing exoplanet census of Mars-sized and sub-Earth planets.

In this paper, we outline the properties of Mars in the context of an exoplanet analog, and its importance in understanding the evolution of planetary processes and surface habitability. Section 2 outlines the major features of Mars in comparison to Earth, and the properties that have played a major role in its evolution and past habitability. Section 3 provides an analysis of the current exoplanet demographics, and example discoveries that may fall into the Mars analog category. Section 4 quantifies the detection limits of exoplanet discovery methods for Mars analogs, including diagnostics of current techniques and predictions for future missions. Section 5 focuses on the habitability prospects of Mars analog exoplanets and their utility in testing the role of various planetary processes that govern the sustainability of temperate surface conditions. Section 6 discusses various implications of Mars for interpreting exoplanet data, and outlines observational discovery strategies optimized for Mars-like exoplanets, with special emphasis on systems hosting Mars-size candidates. We provide concluding remarks and suggestions for future work in Section 7.

2. MARS: FUNDAMENTAL PROPERTIES

Exoplanet studies often use Earth properties as standard units of measurements, particularly for those relevant to describing the capabilities of exoplanet detection methods. Mars has numerous properties that are quite similar to Earth (such as obliquity and rotation rate), and others that substantially diverge (such as mass and surface pressure). Note that the present-day obliquity similarity between Earth (23.44°) and Mars (25.19°) is a snapshot of a chaotic dynamical history; as discussed in

Table 1. Properties of Earth and Mars.

| Property | Earth | Mars |
|----------------------------|-----------|-------|
| Mass (% Earth) | 100 | 11 |
| Radius (% Earth) | 100 | 53 |
| Surface gravity (% Earth) | 100 | 38 |
| Insolation flux (% Earth) | 100 | 44 |
| Solar day (% Earth) | 100 | 103 |
| Surface pressure (% Earth) | 100 | 0.63 |
| Semi-major axis (AU) | 1.00 | 1.52 |
| Obliquity (°) | 23.44 | 25.19 |
| Magnetic field (G) | 0.25–0.66 | ϵ |
| Bond albedo | 0.316 | 0.25 |
| Geometric albedo | 0.43 | 0.17 |
| Moons | 1 | 2 |
| Moon-planet mass fraction | 0.01 | ϵ |

ϵ indicates negligible quantity.

Section 2.2, Mars’ spin-axis tilt has ranged from $\sim 0^\circ$ to $>60^\circ$ on timescales of $\sim 10^5$ – 10^6 yr, meaning the current value is not representative of its long-term climate forcing. Shown in Figure 1 and Table 1 are direct comparisons of Earth and Mars properties, atmospheric composition, interior structure, and various orbital and intrinsic parameters. Examining the commonalities allows an assessment of scaling factors that can aid in both the detection prospects and diagnosis of the potential Earth and Mars exoplanet analogs.

2.1. Formation and Orbit

Isotopic chronometers and dynamical models together suggest that Mars formed rapidly and then stalled at sub-Earth mass because its feeding zone was truncated. Hafnium–tungsten measurements indicate that Mars accreted most of its mass within $\lesssim 2$ – 4 Myr after calcium–aluminum–rich inclusions (CAIs), consistent with a stranded planetary embryo rather than the product of late giant impacts (Dauphas & Pourmand 2011). Two end-member architectures can reproduce the Earth/Mars mass contrast and aspects of the asteroid belt: (i) the Grand Tack, in which Jupiter’s inward migration to ~ 1.5 AU and subsequent reversal depleted solids beyond ~ 1 AU and starved the Mars region (Walsh et al. 2011); and (ii) “annulus” initial conditions that confine most terrestrial material to ~ 0.7 – 1.0 AU, naturally producing an over-massive Earth/Venus and an under-massive Mars (Hansen 2009). Subsequent simulations show that both families of models can match

the Earth/Mars mass ratio while reproducing the belt’s excitation and compositional mixing (Raymond et al. 2009; O’Brien et al. 2014).

Today Mars orbits with semi-major axis $a \simeq 1.5237$ AU, eccentricity $e \simeq 0.0934$, and inclination $i \simeq 1.85^\circ$ (J2000); these values and their uncertainties are provided by modern, refereed planetary ephemerides (e.g., Jet Propulsion Laboratory (JPL) Planetary and Lunar Ephemerides DE440 and DE441) and are consistent over multi-decade fits to spacecraft and radar tracking (Park et al. 2021). Mars’ comparatively large e and i among the terrestrial planets reflect long-term secular forcing dominated by the giant-planet modes, and its orbit undergoes substantial quasi-periodic and chaotic variations in e and i over 10^6 – 10^8 yr (Laskar & Robutel 1993; Laskar et al. 2004). Mars, in turn, exerts its own influence within Solar System dynamical interactions, playing a role within Earth’s Milankovitch cycles (Kane et al. 2025). Ensemble integrations of the full Solar System show that although Mercury can occasionally be driven to extreme eccentricities, the probability of catastrophic inner-planet instability over the next ~ 5 Gyr is at the percent level; Mars remains dynamically long-lived aside from its chaotic secular excursions and strongly chaotic obliquity history (Laskar & Gastineau 2009; Zeebe 2015; Mogavero & Laskar 2021).

2.2. Geological and Climatic Evolution of Mars

Orbital spectroscopy and in-situ analyses show extensive Noachian-age alteration by liquid water: phyllosilicates followed by Hesperian sulfates, consistent with a progressively drying planet. This stratigraphic transition from “phyllosian” to “theikian” provides a time-series of water–rock interaction, pH, and redox conditions (Ehlmann & Edwards 2014; Bibring et al. 2006). The NASA Curiosity rover established that an ancient, long-lived lacustrine system was once present at Gale Crater with neutral pH, low salinity, and essential nutrients—demonstrably habitable for chemolithoautotrophs. The Perseverance rover confirmed a delta–lake system within Jezero Crater, including flood deposits recording hydrologic variability (Grotzinger et al. 2014; Mangold et al. 2021).

Paleomagnetic and crustal remanence data constrain the history of Mars’ global dynamo, though that history is more complex than a simple early cessation. Analyses of Mars Global Surveyor data placed the end of the dynamo in the Noachian, at ~ 4.0 – 4.1 Ga, based on the absence of strong crustal magnetization over the large impact basins Hellas, Argyre, and Isidis (Lillis et al. 2013). However, MAVEN magnetic field measurements over the ~ 3.7 Ga Lucus Planum lava flows reveal confined

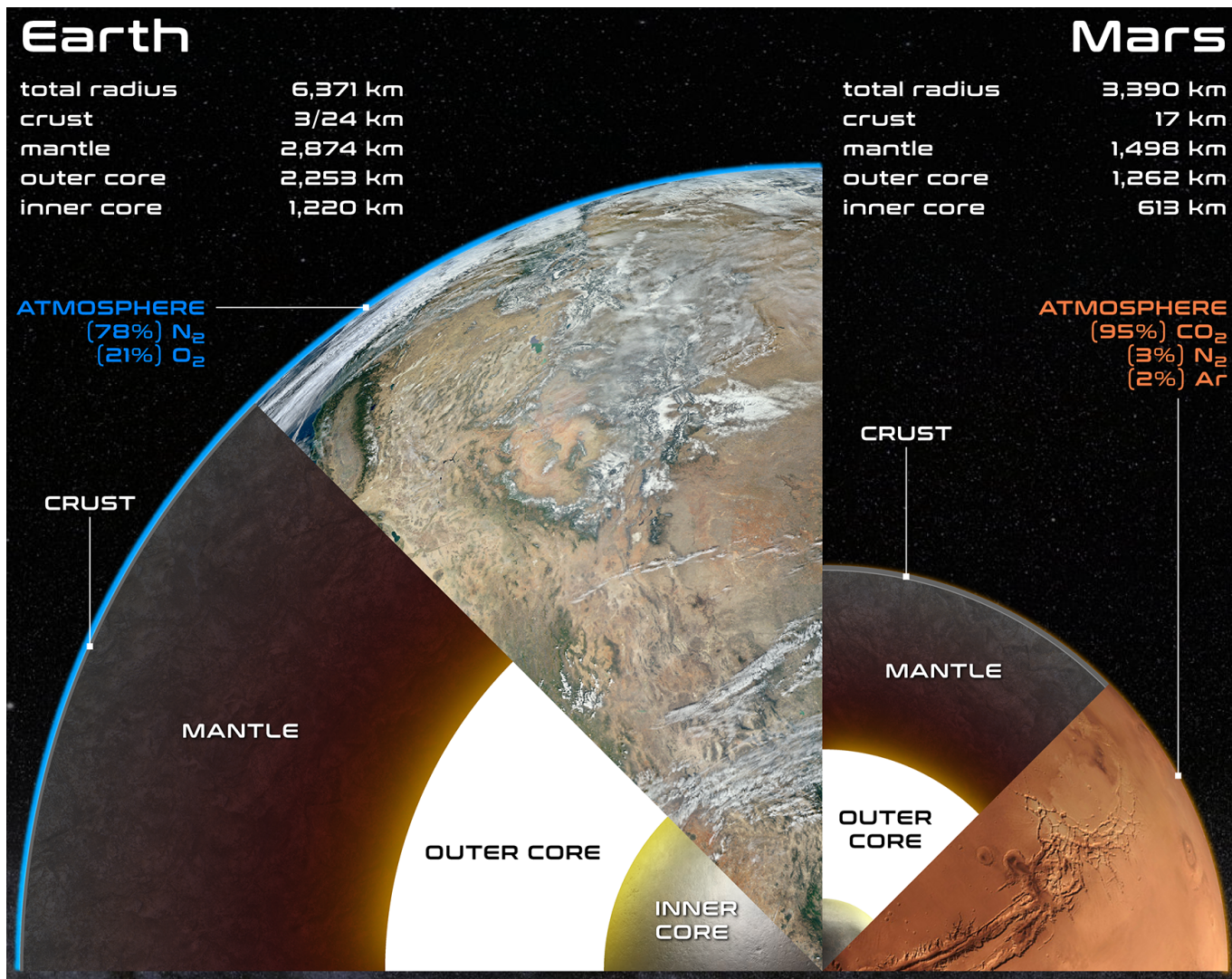


Figure 1. Schematic cross sections of Earth and Mars, showing the major internal components and atmospheric components, to scale. For simplicity, oceanic and continental crust for Earth are not distinguished, nor is the interior structure of Earth's mantle shown.

near-surface magnetization consistent with a dynamo that was active near the Noachian–Hesperian boundary, substantially later than previously thought (Mittelholz et al. 2020). This finding implies that the dynamo may have postdated much of the geomorphic and mineralogic evidence for surface liquid water described above, complicating simple narratives in which dynamo cessation triggers atmospheric loss and climate decline. Furthermore, it remains unclear whether a global magnetic field provides a net protective effect against atmospheric escape. While an intrinsic dipole deflects some solar wind ion pickup, it can also facilitate loss through polar wind outflow and cusp ion escape, such that the presence of a magnetosphere does not guarantee reduced atmospheric erosion (Gunell et al. 2018; Brain et al. 2013). These nu-

ances are important for interpreting exoplanet scenarios where the presence or absence of an intrinsic magnetic field is often assumed to be a binary indicator of atmospheric retention.

Mars undergoes chaotic obliquity variations that modulate insolation distribution, volatile redistribution, and atmospheric pressure via seasonal and long-term CO₂ condensation-sublimation at the poles and regolith (Laskar et al. 1993, 2004). Without a large stabilizing moon comparable to Earth's, Mars' spin-axis tilt has ranged from $\sim 0^\circ$ to $>60^\circ$ on timescales of $\sim 10^5$ – 10^6 yr (Ward 1973; Touma & Wisdom 1993), driving order-of-magnitude swings in polar insolation and seasonal CO₂ cycling (Jakosky et al. 1995; Forget et al. 2006). At high obliquity, polar volatiles migrate toward the equator and

atmospheric mass may temporarily increase, whereas at low obliquity, CO₂ can collapse onto the poles and reduce surface pressure below the triple-point threshold for liquid water. These mechanisms provide a natural laboratory for atmospheric stability thresholds and collapse pathways that offer insights relevant to sub-Earth exoplanets, including tidally locked worlds where qualitatively similar, though dynamically distinct, cold trapping of volatiles can occur (Wordsworth 2015). Mars also exerts its own secular forcing on the inner Solar System, contributing to Earth’s Milankovitch cycles (Kane & Miles 2025), further illustrating how planetary architecture shapes long-term climate evolution.

Mars’ thin CO₂ atmosphere (with O, CO, O₂, N-bearing species, and HOx) is shaped by photochemical cycles that regenerate CO₂ from CO/O and regulate odd-hydrogen chemistry (Nair et al. 1994; Krasnopolsky 2006). The rapid photodissociation of CO₂ by solar UV radiation produces CO and O, but catalytic cycles involving odd-hydrogen species (H, OH, HO₂) efficiently recombine these products and maintain the observed ~95% CO₂ abundance. This balance is sensitive to the water vapor profile, dust loading, and UV flux (parameters that vary with orbital state and atmospheric dust events) making the Martian photochemical system a real-world testbed for photochemical models of thin CO₂ atmospheres on rocky exoplanets (Lefèvre & Forget 2009). In the exoplanet context, Mars photochemistry constrains the production rates of abiotic O₂ and O₃, which are key false-positive biosignature gases expected on irradiated, low-outgassing worlds. The Martian example also provides empirical constraints on the thermodynamic conditions under which CO₂ condensation occurs, which are relevant to the nightside cold traps of tidally locked exoplanets, where the atmospheric circulation regime and heat-transport efficiency introduce additional controls on collapse thresholds (Wordsworth 2015).

2.3. Atmospheric Loss: Mechanisms and Constraints

The present-day Martian atmosphere provides direct evidence that small rocky planets are highly susceptible to long-term volatile loss. Although the present atmosphere of Mars is relatively thin, the early atmosphere was likely far more substantial, since that is required to account for the hosting of surface liquid water (Pollack et al. 1987; Jakosky & Phillips 2001; Wordsworth 2016; Kite 2019; Warren et al. 2019). For example, Joiret et al. (2025) estimated a conservative minimal mass of the primordial Martian atmosphere that implies a surface pressure of at least 2.9 bar. This primordial atmosphere, present during and immediately following plan-

etary formation, was itself shaped by early volatile processing including hydrodynamic escape during magma-ocean stages, isotopic exchange between the atmosphere and solidifying mantle, and impact-driven loss and delivery (Pepin 1991; Kasting 1993; Elkins-Tanton 2008; Pahlevan & Stevenson 2007). The subsequent atmosphere that hosted the surface liquid water recorded in the geologic record (beginning ~4.0–4.3 Ga) may have differed substantially from this primordial state.

More broadly, the atmospheric evolution of any planet depends critically on the initial volatile inventory incorporated during formation, which in turn reflects the composition, location, and timing of accreting materials (Jakosky & Treiman 2023). Given that the initial incorporation of volatiles into planets remains poorly understood even within our own Solar System (where we have extensive observations of planets, asteroids, and meteorites) the range of possible atmospheric outcomes for Mars-sized exoplanets with unknown formation histories is correspondingly large. This uncertainty in initial conditions must be borne in mind when extrapolating from Mars to exoplanet populations.

Lyman- α observations and analyses of combined data from MAVEN and the Emirates Mars Mission (EMM) reveal that hydrogen escape—often diffusion-limited—can be seasonally or dust-storm enhanced; large dust events correlate with spikes in upper-atmosphere H and increased escape, demonstrably linking climate and loss (Chaffin et al. 2014; Heavens et al. 2018; Chaffin et al. 2021). Recent observations from MAVEN have provided direct quantitative constraints on the dominant non-thermal escape pathways operating at Mars today, helping to anchor escape models for small exoplanets subjected to elevated XUV and stellar winds. For example, measurements of ion escape rates indicate that atmospheric loss is strongly modulated by solar wind conditions, including dynamic pressure and interplanetary magnetic field orientation, with significant enhancements observed during space weather events such as coronal mass ejections (Jakosky et al. 2015, 2018). MAVEN observations further demonstrate that pickup ion escape, in combination with solar wind-driven sputtering, represents an ongoing mechanism for atmospheric erosion in the absence of a global magnetic dynamo (Brain et al. 2016). Additionally, photochemical escape of oxygen, driven by dissociative recombination of O₂⁺ in the upper atmosphere, currently exceeds ion escape as an O loss channel and can operate regardless of whether a global dynamo is present (Lillis et al. 2017).

Enrichment of heavy isotopes (³⁸Ar/³⁶Ar, D/H, ¹⁵N/¹⁴N) from in-situ measurements indicates substan-

tial atmospheric loss by mass-selective processes [Jakosky et al. \(2017\)](#). Such isotopic forensics calibrate retrieval expectations for exo-atmospheres once precision spectroscopy becomes feasible ([Mahaffy et al. 2013](#); [Webster et al. 2013](#)). Early Mars likely experienced hydrodynamic H escape during magma-ocean/outgassing phases ([Pepin 1991](#); [Tian et al. 2009](#)) and episodic atmospheric loss due to large impacts ([Melosh & Vickery 1989](#)); both processes leave distinct isotopic and volatile-inventory signatures relevant to young exoplanets. These results suggest that episodic climate variability may contribute to long-term volatile depletion and provide an empirical benchmark for evaluating atmospheric retention on Mars analog exoplanets, particularly those orbiting active stars with elevated stellar wind fluxes ([Brain et al. 2026](#)).

2.4. Past Habitability: Duration and Conditions

Liquid water is the essential solvent for life as we know it, and the history of its abundance on Mars is central to assessing planetary habitability. The past presence of water, and thus potential habitable environments, is recorded in the Martian geologic record through geomorphological features such as catastrophic outflow channels, fluvial channel systems and valley networks, sedimentary fan deposits, and features potentially consistent with a former ocean. These geomorphological indicators are strongly supported by orbital spectral observations that reveal a wide variety of hydrated minerals and mineraloids, including Fe/Mg-smectite clays, chlorites, kaolinite, mica, hydrated silica, zeolites, sulfates, serpentine, and carbonates. Together, these mineral assemblages indicate widespread and diverse water-rock interactions over Mars’ history (e.g., [Bibring et al. 2006](#); [Milliken et al. 2008](#); [Mustard et al. 2008](#); [Ehlmann et al. 2009, 2010, 2011](#); [Wray & Ehlmann 2011](#)), with Fe/Mg-smectite clays being the most abundant, followed by chlorites.

Longer-lived and widespread liquid water on Mars most likely occurred during the pre-Noachian to Noachian periods. Shorter-lived episodes of liquid water at the surface and in the subsurface, along with associated water-rock interactions, likely persisted into the Hesperian and Amazonian periods and may have formed protected or transient habitable environments ([Cockell 2014](#); [Westall et al. 2015](#)). Specifically, sedimentologic facies and geochemical characteristics at both ongoing rover missions sites show that lakes at Gale crater and deltas at Jezero crater persisted for at least centuries to millennia (likely longer), with redox couples (Fe/S) and nutrients sufficient for microbial metabolisms. The preservation potential of fine-grained mudstones and

deltaic foresets informs taphonomic criteria for future biosignature searches on exoplanets (e.g., depositional “traps” inferred from global photometry and spectra) ([Grotzinger 2014](#); [Mangold 2021](#)).

In addition to lacustrine settings, hydrothermal environments represent prime targets in the search for biosignatures, as they provide sustained heat and liquid water and can concentrate biological materials. Moreover, the highest potential for biosignature preservation is found in geologic materials that experienced limited diagenesis and metamorphism, minimizing overprinting of primary signatures (e.g., [Sun & Milliken 2018](#); [Voigt et al. 2024](#); [Millan et al. 2025](#), Opal-A), as well as limited exposure to the Martian surface and atmosphere, where oxidizing conditions and radiation would otherwise degrade or destroy the initial signature. The taphonomic criteria established by Mars exploration (particularly the preservation potential of fine-grained mudstones, deltaic foresets, and hydrothermally altered materials) provide a transferable framework for identifying high-priority biosignature targets on rocky exoplanets, where analogous depositional “traps” might be inferred from disk-integrated photometry and spectra.

3. EXOPLANET DEMOGRAPHICS

As an exoplanet analog, Mars has numerous properties and processes that are directly translatable to diagnosing planetary evolution in a general planetary framework. For example, CO₂ frost cycling, radiative-dynamical coupling in a tenuous atmosphere, and dust-radiation feedbacks constrain climate stability models for tidally locked terrestrial exoplanets, testing predictions of CO₂ atmospheric collapse thresholds ([Wordsworth 2015](#)), although the dynamical regimes differ and such extrapolations carry inherent uncertainties associated with boundary conditions and processes that may not be captured by models validated only under present-day Martian conditions. Empirical atmospheric escape rates under weak gravity, and their XUV/wind dependencies, partially calibrate models for small exoplanets, including those around active M-dwarfs where non-thermal processes can dominate, though the substantially harder XUV spectra and more variable flaring environments of M-dwarfs shift the relative weights of escape channels in ways that Mars alone cannot fully constrain ([Jakosky et al. 2018](#); [Brain et al. 2026](#)). Noble-gas and hydrogen isotope fractionation under known escape regimes calibrate how we read future high-precision spectra of small exoplanet atmospheres ([Mahaffy et al. 2013](#)). Furthermore, Mars’ photochemistry (CO/CO₂/O₂/O₃/HOx) constrains oxidation states and potential false positives (abiotic O₂/O₃) expected on ir-

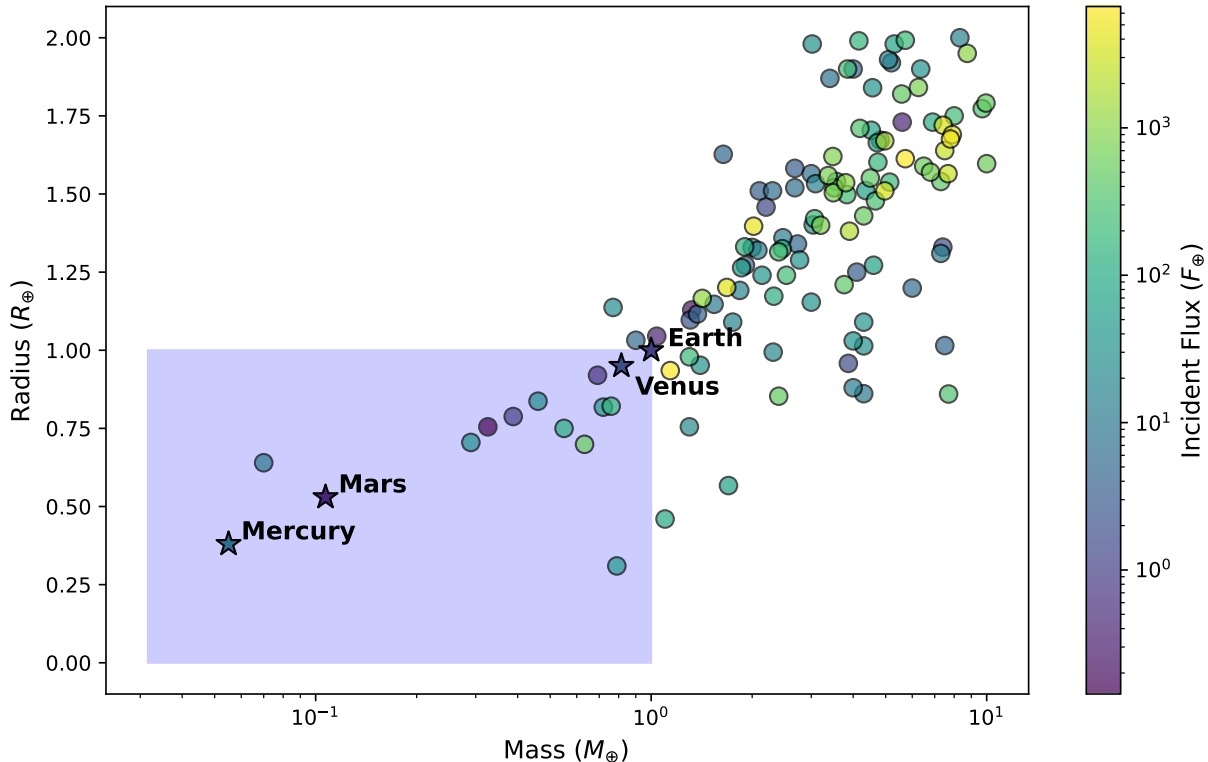


Figure 2. Planetary mass and radius data for those confirmed exoplanets that have measurements extracted for both properties, extracted from the NASA Exoplanet Archive on 2025, December 31. The data are color-coded in proportion to the flux received from their host stars. The Solar System terrestrial planets are shown as stars. The shaded region indicates the sub-Earth regime, defined as $M_p < 1 M_\oplus$ and $R_p < 1 R_\oplus$.

radiated, low-outgassing exoplanets (Lefèvre & Forget 2009).

Empirical mass-radius measurements for small exoplanets provide the critical mapping from the radius-rich transit census to physically interpretable masses, bulk compositions, and volatile fractions (Dorn et al. 2015; Unterborn et al. 2023). However, the terrestrial regime remains strongly data-limited once one requires both the mass (M_p) and radius (R_p) of the planet. Shown in Figure 2 are the mass and radii for all confirmed exoplanets with reported masses of $M_p \leq 10 M_\oplus$ and radii of $R_p \leq 2 R_\oplus$, as extracted from the NASA Exoplanet Archive on 2025, December 31 (Christiansen et al. 2025). The query includes all planets with non-null mass and radius entries regardless of measurement provenance (RV, TTV, or other), and no explicit precision cut is applied; we note that the demographic shape in Figure 2 is sensitive to the inclusion of lower-precision TTV-derived masses. This yielded a total of 120 exoplanets, shown in Figure 2 as data points that are color-coded by the calculated flux received by the planet (F_p). We also include the Solar System terrestrial planets, shown as stars. The shaded region indicates the area

of mass-radius space that is sub-Earth in value, and includes 11 exoplanets: TRAPPIST-1 h, TRAPPIST-1 e, TRAPPIST-1 d, Kepler-138 b, L 98-59 b, K2-266 c, Kepler-37 b, HD 23472 e, HD 23472 d, Kepler-20 e, and GJ 367 b. A subset of these 11 exoplanets have been monitored using the transmission spectroscopy capabilities of JWST or the Hubble Space Telescope (HST), with no evidence found for the presence of substantial atmospheres (Damiano et al. 2022; Zhang et al. 2024; Glidden et al. 2025; Piaulet-Ghorayeb et al. 2025).

The relative scarcity of data within the shaded region is not necessarily evidence that Mars analogs are intrinsically rare; rather it is an imprint of survey selection effects. Transit surveys, such as Kepler (Borucki 2016), preferentially populate the observed M_p - R_p plane at short periods and high F_p because the geometric transit probability scales roughly as R_\star/a , where a is the orbital semi-major axis. Furthermore, detectability requires sufficient signal-to-noise and multiple observed transits, driving completeness sharply downward for sub-Earth radii at long periods (Kane & von Braun 2008; Borucki et al. 2010; Mulders et al. 2018). Occurrence-rate analyses that correct for these effects demonstrate

that small planets are common in radius space (Fressin et al. 2013; Dressing & Charbonneau 2015), yet these radius-based demographics do not readily translate into a mass-defined Mars frequency (Mulders et al. 2018). Thus, the sub-Earth (shaded) portion of Figure 2 is disproportionately anchored by highly irradiated transiting planets around low-mass stars and/or by transit-timing variations (TTVs) in compact, near-resonant architectures (Howard et al. 2010; Rogers 2015; Winn & Fabrycky 2015).

Even so, there are already several candidate systems in (or near) the Mars-size domain that serve as potential testbeds for Mars analogs in radius, though their orbital and irradiation environments differ substantially from Mars. The ultra-compact Kepler-42 (KOI-961) system hosts three sub-Earths including a Mars-sized planet ($R_p \approx 0.57 R_\oplus$) (Muirhead et al. 2012). Kepler-444 contains five sub-Earths with radii spanning roughly Mercury to sub-Venus sizes (Campante et al. 2015). Kepler-37 includes a Moon-to-sub-Earth sequence and a $\sim 0.74 R_\oplus$ planet that lies between Mars and Earth in size (Barclay et al. 2013). The mass of the Mars-sized exoplanet Kepler-138 b was determined via TTVs, further demonstrating the challenge in establishing the properties of sub-Earth size planets (Jontof-Hutter et al. 2015). More recently, the nearby L 98–59 system features a transiting $\sim 0.84 R_\oplus$ planet plus additional terrestrial companions with precise masses and radii, enabling comparative studies of interior-atmosphere diversity at sub-Earth scales (Demangeon et al. 2021). Furthermore, the validated Mars-size planet candidate KOI-4777.01 presents an interesting case of how such planets evolve in extreme flux environments around an M-dwarf (Cañas et al. 2022). These systems exemplify target classes where Mars-derived priors on volatile budgets, photochemistry, and escape histories can be quantitatively exercised against current and forthcoming observations.

4. DETECTING MARS EXOPLANET ANALOGS

Here we discuss prospects for detecting Mars exoplanets analogs, and the potential for characterization of their properties and atmospheres.

4.1. *Transits*

The transit technique of exoplanet discovery has thus far detected the vast majority of known exoplanets (Christiansen et al. 2025). The photometric depth induced by a planetary transit scales as a simple relationship between the radius of the planet and host star, as: $\delta \approx (R_p/R_\star)^2$. For example, a Mars-size ($R_p \approx 0.53 R_\oplus$) planet transiting a late M-dwarf host

star ($R_\star \approx 0.12 R_\odot$) will yield a transit depth of $\delta \sim 1.6 \times 10^{-3}$, or ≈ 1600 ppm. Although a transit signature of this amplitude is readily accessible from both ground and space-based facilities, such a planet-star configuration represents the best-case scenario. A Mars-size planet transiting K dwarf ($R_\star \approx 0.7 R_\odot$) or G dwarf ($R_\star \approx 1.0 R_\odot$) host star will yield transit depths of 49 ppm and 24 ppm, respectively. Such transit depths are challenging even from space-based photometry, particularly in the face of intrinsic stellar variability (Aigrain et al. 2004; Ciardi et al. 2011; Morris et al. 2020; Fetherolf et al. 2023). However, as described in Section 3, several transiting Mars-size planets have indeed been detected, albeit within the high incident flux regime where mass measurements are enabled via radial velocities (RVs) or TTVs within systems where orbital resonance is present (Grimm et al. 2018; Agol et al. 2021).

The detection of true Mars analogs (at relatively low flux) will face the challenge of building up signal-to-noise over multiple transits over an extended period. Although results from the Transiting Exoplanet Survey Satellite (TESS) have significantly added to the known inventory of small planets around M-dwarfs, the 27-day sectors observations decreases sensitivity to longer period planets (Ricker et al. 2015; Kane et al. 2021c; Brady & Bean 2022). On the other hand, the upcoming PLANetary Transits and Oscillations of stars (PLATO) mission is designed for long-baseline, high-precision photometry on bright nearby stars (Rauer et al. 2014, 2025). PLATO will continuously monitor selected fields for 2–3 years, enabling detection of terrestrial planets with much longer orbital periods than those represented in the TESS inventory, including Earth analogs around Sun-like stars and potentially planets in the outer HZs of M-dwarfs. By extending transit searches to periods of ~ 1 year or longer, PLATO will complement the results of the Kepler and TESS missions, and may yield systems of multiple transiting terrestrial planets in strong resonance configurations (Heller et al. 2022; Matuszewski et al. 2023; Boettner et al. 2024).

4.2. *Radial Velocities*

Many of the initial exoplanet detections were the result of RV observations through spectroscopic observations of bright stars in the solar neighborhood (Butler et al. 2006; Schneider et al. 2011; Christiansen et al. 2025). The push towards RV precisions that enable terrestrial exoplanet detection has required the evolution of Extreme Precision RVs (EPRVs) and the diagnosis of contamination from stellar activity (Saar & Donahue 1997; Fischer et al. 2016; Vanderburg et al. 2016; Cale

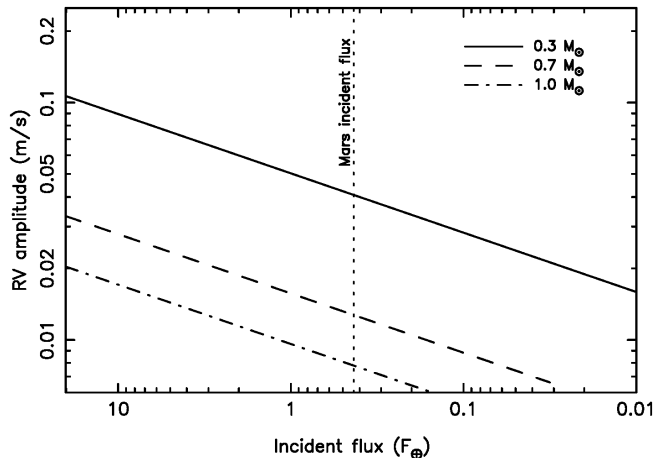


Figure 3. Predicted RV amplitude for a Mars-mass exoplanet as a function of incident flux, where the vertical dotted line indicated the incident flux for Mars ($\sim 0.43 F_{\oplus}$). The calculations are shown for host stars of mass 0.3, 0.7, and $1.0 M_{\oplus}$.

et al. 2021). Numerous EPRV instruments have been developed and deployed, with most aiming for precisions better than ~ 50 cm/s over long periods of observation (Gibson et al. 2016; Jurgenson et al. 2016; Schwab et al. 2016; Seifahrt et al. 2016; Pepe et al. 2021).

The RV amplitude of the Sun due to the gravitational influence of Mars is $K \sim 7.8$ mm/s, which is substantially beyond the reach of current EPRV instruments. By comparison, the RV amplitude induced on the Sun by Earth is $K \sim 8.9$ cm/s. Figure 3 shows the maximum (edge-on orbit) predicted RV amplitude for a Mars-mass planet in a circular orbit as a function of incident flux for three different host stars: an M-dwarf (solid line), a K-dwarf (dashed line), and a G dwarf (dot-dashed line). The RV amplitude for a Mars-mass planet at Mars equivalent flux around a K dwarf and M-dwarf are $K \sim 1.3$ cm (~ 0.815 AU) and $K \sim 4.1$ cm/s (~ 0.185 AU), respectively. In order for a Mars-mass planet to produce a similar RV amplitude to an Earth analog requires a flux of $10 F_{\oplus}$ when orbiting an M-dwarf. Thus, the most promising near-term opportunity for the RV detection of Mars-mass planets requires targeting low-mass stars and short orbital periods.

4.3. Astrometry

The astrometric method of exoplanet detection, relying on precise measurements of stellar positions, has advanced considerably in recent years, primarily through the data releases from the Gaia mission (Perryman et al. 2014; Brandt 2018, 2021; Gaia Collaboration et al. 2021). For example, the Gaia data have been used to refine the measured properties of known exoplanets and

their host stars (Stassun et al. 2017; Berger et al. 2018; Fulton & Petigura 2018; de Laverny et al. 2025) and have demonstrated that some previously detected RV companions do not lie in the planetary-mass regime (Kiefer 2019).

The semi-amplitude of the astrometric effect scales linearly with the semi-major axis and mass of the planet, and thus favors massive planets at large separations from the host star. For example, a Neptune/solar analog located at a distance of 35 pc would produce an astrometric semi-amplitude of $44 \mu\text{arcsec}$ (Kane 2011), or $154 \mu\text{arcsec}$ if located at 10 pc. By comparison, a Mars/solar analog located at 10 pc would induce a maximum astrometric semi-amplitude of only 49 nas. A Mars orbiting at Mars-equivalent flux around a K-dwarf and M-dwarf, also at 10 pc, would induce maximum astrometric semi-amplitudes of ~ 37 nas and ~ 20 nas, respectively. Thus, a Mars analog at 10 pc will produce an astrometric signature that lies considerably below the noise floor of Gaia ($\gtrsim 10\text{--}20 \mu\text{as}$) or any currently planned astrometric mission.

4.4. Gravitational Microlensing

Gravitational microlensing probes exoplanets through the transient magnification of a background “source” star as a foreground “lens” system closely aligns with the line of sight. In the planetary regime, the observable signature is a short-lived perturbation to an otherwise smooth point-lens light curve (Paczynski 1986; Mao & Paczynski 1991; Gould & Loeb 1992; Paczynski 1996; Gaudi 2012). Microlensing is particularly sensitive to cold planets on wide orbits (typically near the Einstein-ring scale) and to planetary systems at kpc distances (Albrow et al. 2001; Cassan et al. 2012; Gaudi 2012). This regime naturally includes terrestrial and sub-terrestrial planets in Mars-mass bins, provided that the planetary perturbation is sufficiently well sampled and not erased by finite-source effects.

Modern ground-based microlensing planet searches rely on wide-field, high-cadence monitoring of the crowded Galactic bulge from multiple longitudes. Major survey facilities include the Optical Gravitational Lensing Experiment (OGLE-IV) (Udalski et al. 2015), the Microlensing Observations in Astrophysics survey (MOA-II) (Sako et al. 2008), and the Korea Microlensing Telescope Network (KMTNet) (Kim et al. 2016). Despite these advances, detecting Mars analogs from the ground remains difficult for three related reasons: (i) the intrinsic rarity of microlensing alignments (necessitating very large monitored star counts), (ii) the relatively short duration of low-mass planetary perturbations, and (iii) systematic and sampling limitations from

atmospheric seeing, blending in dense fields, weather, and diurnal gaps (Gaudi 2012; Zang et al. 2025). In particular, small-planet anomalies can be missed or poorly constrained when data are interrupted during the perturbation (Zang et al. 2025). Even so, the ground-based low-mass frontier is approaching the Earth-mass regime in favorable (typically high-magnification) events. For example, Zang et al. (2021) reported KMT-2020-BLG-0414Lb with a planet-host mass ratio $q \sim 10^{-5}$. By contrast, Mars analogs around typical bulge lenses ($0.3 M_{\odot}$ at 6 kpc) correspond to $q \sim 10^{-6}$, where the signal timescale shrinks and the detection cross-section drops by an additional factor $\sim \sqrt{10}$. Consequently, present ground-based statistical constraints on cold-planet demographics are best developed at higher mass ratios rather than at Mars-like ratios.

The Nancy Grace Roman Space Telescope will conduct a dedicated Galactic Bulge Time-Domain Survey (GBTDS) with a high-cadence, near-infrared wide-bandpass sequence designed explicitly for microlensing demographics, including sensitivity to low-mass planets (Sajadian 2021; Fatheddin & Sajadian 2023). Space-based observations address the principal ground limitations by providing weather-free, high duty cycle during observing seasons, stable point-spread functions and calibrated photometry, and substantially reduced crowding/blending relative to typical ground seeing (Gaudi 2012; Terry et al. 2025). Roman yield forecasts discuss total event samples of order $\sim 5 \times 10^4$ microlensing events over the nominal six-season survey, depending on the event definition and impact-parameter cut (Saggese et al. 2025). Forecasts further indicate that Roman is expected to detect bound planets above $\sim 0.1 M_{\oplus}$ (i.e., Mars mass) in statistically useful numbers and maintain sensitivity down to $\sim 0.02 M_{\oplus}$ under favorable circumstances (Penny et al. 2019). Overall, gravitational microlensing remains one of the most promising techniques for discovering cold, low-mass exoplanets at wide separations, with the caveat of relatively brief planetary deviations requiring sufficient observational cadence to characterize the planetary system.

4.5. Direct Imaging and Thermal Emission

Current ground-based direct-imaging surveys remain fundamentally optimized for young, self-luminous giant planets rather than cold Mars analogs. Even with extreme Adaptive Optics (AO), coronagraphy, and modern post-processing, survey-grade near-IR performance is typically in the $\sim 10^{-6}$ – 10^{-7} contrast regime at arc-sec separations (Chomez et al. 2025). Demographic constraints from large ground surveys therefore concentrate on companions of a few to $\gtrsim 10 M_J$ at multi-AU to

~ 100 AU scales, not on sub-Earth rocky planets (Nielsen et al. 2019). For calculating the planet-star flux ratio of Mars analogs in reflected light, we adopt the formalism of Kane & Gelino (2010, 2011a). Assuming a geometric albedo of $A_g = 0.15$, a planetary radius of $R_p = 0.53 R_{\oplus}$, a semi-major axis of $a = 1.52$ AU, and a Lambertian reflectance, we calculate a planet-star flux ratio of $\epsilon = 1.1 \times 10^{-11}$, which is several orders of magnitude fainter than present contrast floors. Thermal emission has a less demanding intrinsic contrast (Marley et al. 1999; Sudarsky et al. 2000; Kane & Gelino 2011b; Guzewich et al. 2020), which, for a temperate Mars analog around a solar twin, is of order $\sim 10^{-8}$ near wavelengths of $10 \mu\text{m}$, but ground-based sensitivity at thermal-IR wavelengths is critically limited by high thermal backgrounds (Rousseau et al. 2024).

Future space-based, high-contrast observatories are expected to shift toward the feasibility of Mars-analog detectability with the Habitable Worlds Observatory (HWO), explicitly conceived as a large UV/optical/IR facility designed to directly image and spectroscopically characterize potentially habitable planets (Harada et al. 2024; Kane et al. 2024; Stark et al. 2024b; Tuchow et al. 2024). Post-processing frameworks and operations concepts for a HWO-class coronagraph are being developed around the need to measure flux ratios of $\sim 10^{-11}$ (McElwain et al. 2025). For a Sun-like star at $d = 10$ pc, a Mars-orbit analog has an angular separation of $\theta = 0.152''$, which is outside the anticipated visible-light Inner Working Angle (IWA). However, a robust detection will require a substantially deeper search than for an Earth analog, as the reflected light flux ratio of a Mars analog ($\epsilon \sim 10^{-11}$) is roughly an order of magnitude fainter than for an Earth analog ($\epsilon \sim 10^{-10}$), requiring correspondingly longer integration times. This implies that Mars-analog yields will likely be driven by targeted deep observations of the nearest and most favorable stars rather than uniform completeness across the full exoEarth sample (Stark et al. 2024a). Stellar-type and distance trade-offs may be considered, meaning late-type stars offer higher reflected-light contrast but smaller angular separations. These couplings motivate yield optimization (and wavelength/IWA trade studies) as the operational path to recovering Mars-analog completeness once HWO-class stability and contrast are achieved (Stark et al. 2024a). A dedicated mid-IR space interferometer, such as the Large Interferometer For Exoplanets (LIFE), would greatly expand the search domain, enabling detection/characterization of hundreds of small planets, including potential Mars analogs (Quanz et al. 2022).

4.6. Atmospheric Characterization

Atmospheric characterization of Mars-like exoplanets is scientifically compelling because even a tenuous CO₂-rich atmosphere can profoundly affect surface habitability and attest to a planet’s volatile history (Tinetti et al. 2005; Wolfe & Robinson 2024). Alternatively, the lack of a substantial atmosphere may be consistent with strong escape mechanisms dominating over the atmospheric evolution, as has been inferred from JWST observations in several cases (Greene et al. 2023; Zieba et al. 2023). For example, a positive detection of H₂O, O₃, or other photochemical tracers may indicate remnant oceans or past high-energy irradiation, providing key benchmarks for comparative planetology (Schwieterman et al. 2018; Fujii et al. 2018; Ostberg et al. 2023). To investigate the observable signatures, we simulated transmission and reflectance spectra of a Mars analog using the Planetary Spectrum Generator (PSG; Villanueva et al. 2018). Each model uses the same Martian planetary configuration. The model utilizes a surface pressure and temperature of ~ 6 mbar and ~ 216 K, respectively. The bulk composition of the model atmosphere is dominated by CO₂ (96.934%), with N₂ (1.897%) and O₂ (0.144%) as secondary constituents, and trace amounts of CO, H₂O and O₃. The model atmosphere also includes two aerosol species; dust (2.921 ppm) and water ice (0.947 ppm), both of which have particle radii of $1.222 \mu\text{m}$ (Millour et al. 2015, 2024). These aerosols, along with the surface albedo ($A = 0.2448$) and emissivity ($\epsilon = 0.7555$) are wavelength-dependent, and the spectral signature’s detectability is influenced by the spectral energy distribution of the host star (Shields et al. 2016; Wunderlich et al. 2019). For solar-type stars, reflected light dominates at shorter wavelengths, meaning that there are stronger signals occurring at shorter wavelengths. On the other hand, M-type stars dominate in the near-IR, and will therefore have stronger features in that wavelength regime. This also means that surface and atmospheric features in the near-IR will become more prominent compared to that of a solar-type star. We note that these parameters are specific to present-day Mars, and that variations in surface pressure, albedo, or atmospheric composition (as might arise under different stellar spectra or earlier evolutionary states) would affect the depth and detectability of spectral features. For example, increasing the dust opacities could raise the effective albedo and reduce emission feature depths, while increasing the pressure would broaden CO₂ absorption features and enhance transmission signals.

Figure 4 shows the simulated transmission spectrum of a Mars analog around a Sun-like star at a distance of 10 pc, over a wavelength range of 0.2–10 μm (modeled

on JWST/NIRSpec PRISM). The left and right vertical axes shows the depth of the absorption features for a G2 dwarf host and an M5 dwarf host, respectively. Strong CO₂ absorption features appear at 2.7 and 4.3 μm , in analogy to those seen in Earth’s spectrum, and span several atmospheric scale heights. The corresponding transit depth variation is extremely small: $< 10^{-6}$ for a Mars-size planet and Sun-like star, making detection challenging even with JWST. Indeed, Kreidberg & Stevenson (2025) noted that rocky exoplanet spectra require multi-scale-height features for firm detections. Figure 4 demonstrates that, aside from the strongest bands, most absorption features remain near or below the noise floor, reflecting the high mean molecular weight and compact atmosphere of Mars analogs (Lustig-Yaeger et al. 2023; Rigby et al. 2023).

Direct imaging in reflected light offers complementary spectral information. Figure 5 displays model reflected spectra of a Mars analog observed at phase angles of 0°, 90°, and 135°, at a distance of 10 pcs, and assuming a 15 m coronagraph-equipped telescope over 0.2–10 μm (Kawashima & Rugheimer 2019), based approximately on the Large Ultraviolet Optical Infrared Surveyor (LUVOIR) A-VIS instrument (The LUVOIR Team 2019). The reflected spectra in Figure 5 show modest signatures of CO₂ and surface mineral bands, with overall brightness declining at larger phase angles. As noted by Rocetti et al. (2025b), reflected-light spectra as a function of wavelength and phase angle encode atmospheric and surface properties (e.g., albedo variations and molecular absorptions such as O₂, H₂O, CH₄, CO₂). By comparing the three spectra in Figure 5, the full-phase (0°) spectrum is approximately uniformly bright across wavelength, while at 90°–135° the absorption features are weaker and the flux falls sharply at NIR wavelengths due to the reduction in Rayleigh and forward Mie scattering (Rocetti et al. 2025b,a). These variations can be exploited to retrieve composition: for example, deep CO₂ bands at 4.3 μm and weaker H₂O or O₃ features will modulate the reflected color differently from bare surface (García Muñoz & Cabrera 2018). Thus, direct imaging at HWO-class contrasts ($\sim 10^{-10}$) is expected to yield more abundant molecular information for nearby Mars analogs than transit spectroscopy alone.

5. HABITABILITY OF MARTIAN ANALOGS

The long-term habitability of Mars-size exoplanets is controlled by how quickly small rocky bodies cool, degas, and then lose their atmospheres (Unterborn et al. 2022; Hill et al. 2026). As planetary radius decreases, the smaller volume to surface area ratio allows conduc-

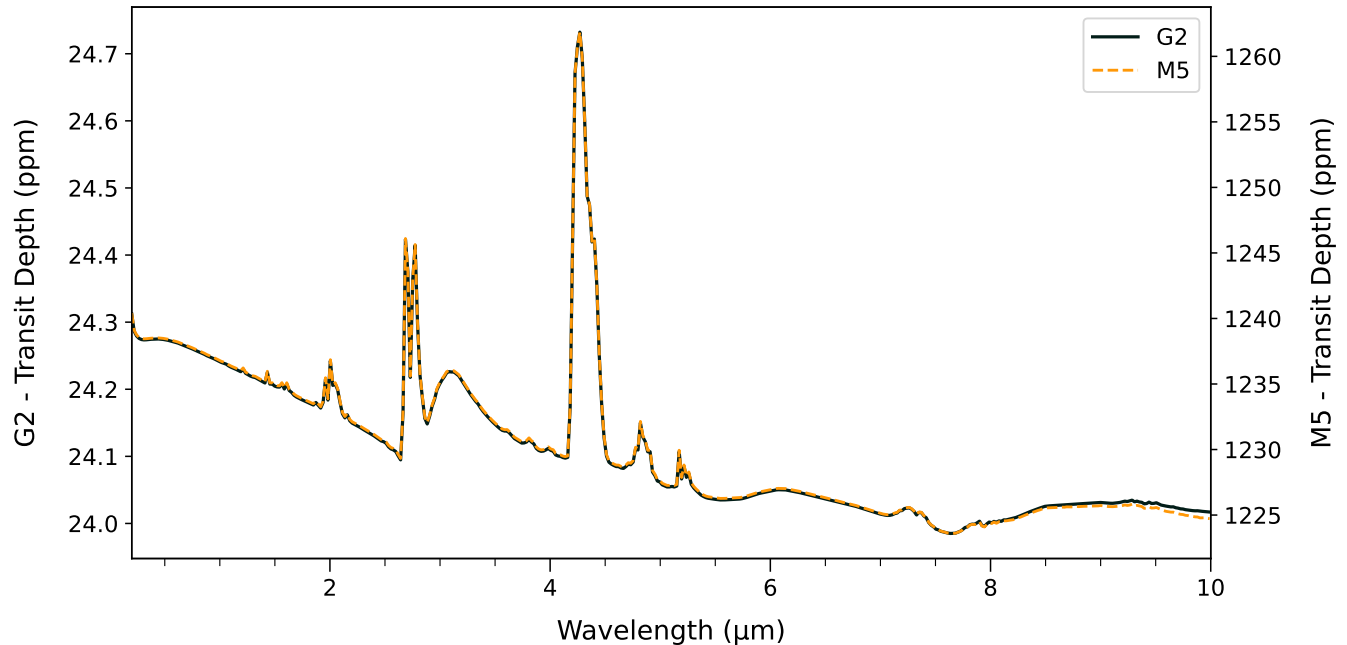


Figure 4. Transmission spectrum of a Mars analog in an edge-on orbit around a host star located at a distance of 10 pc. The left and right vertical axes show the strength of the absorption features for a G2 dwarf and M5 dwarf host star, respectively.

tive cooling to occur more quickly, as too does a reduction in radiogenic materials correlated to the mantle mass reduction of the planet. This cooling has the effect of reducing convective vigor and decreasing melt production, both of which may contribute to whether the planet is able to start and/or maintain plate tectonics (O’Neill & Lenardic 2007; Grott et al. 2011; Unterborn et al. 2022). Analysis of Mars mantle volatile abundances and atmospheric inventories supports these theoretical predictions, demonstrating that initial volatile budgets and subsequent outgassing histories are critical controls on long-term atmospheric mass (Jakosky & Treiman 2023). In such bodies, most volatile release occurs early, during magma–ocean solidification and the first few hundred Myr of mantle overturn, followed by an order-of-magnitude (or more) reduction in outgassing rates after $\sim 0.5\text{--}1.5$ Gyr as reducing mantle temperatures prohibit melt production (Noack et al. 2017; Tosi et al. 2017). Whether degassing can persist depends on the efficiency of melt focusing through a thick, dehydrated lithosphere and on the availability of carbonate reservoirs, and models generally predict shorter-lived volcanic-degassing epochs for Mars-mass planets than for Earth analogs (Foley & Smye 2018; Grott et al. 2011). These model predictions are consistent with the volcanic history of Mars compared with, for example, that of Earth (Byrne 2020). These interior trends also couple to magnetic evolution: small cores cool rapidly,

so dynamos are typically brief, potentially further exposing atmospheres to stellar wind erosion once magnetism wanes (Driscoll & Bercovici 2013; Lillis et al. 2013; Gunell et al. 2018).

Atmospheric retention on Mars-size worlds is therefore a race between supply (early and episodic volcanism, impacts) and loss (thermal and non-thermal escape). High XUV irradiation drives hydrodynamic escape of H (and in extreme cases, drag-off of heavier species), with escape efficiencies that peak during the first $10^8\text{--}10^9$ yr when stars are most active (Tian 2009; Murray-Clay et al. 2009). Non-thermal processes (ion pickup, sputtering, and photochemical escape) become dominant once the upper atmosphere is H-poor, especially without a persistent magnetosphere (Jakosky et al. 2018). Around active M-dwarfs, the extended pre-main-sequence luminosity plateau and strong space weather (flares, CMEs, winds) can desiccate and erode secondary atmospheres. For example, simple energy-limited estimates imply loss of multiple terrestrial ocean equivalents in $\lesssim 100$ Myr for close-in orbits unless outgassing is exceptionally vigorous or shielding is strong (Luger & Barnes 2015; Airapetian et al. 2017; Dong et al. 2018a; Bolmont et al. 2017). In addition, thin CO_2 atmospheres on tidally locked planets can collapse into cold traps if heat transport and background pressure are insufficient, setting a CO_2 -stability floor that

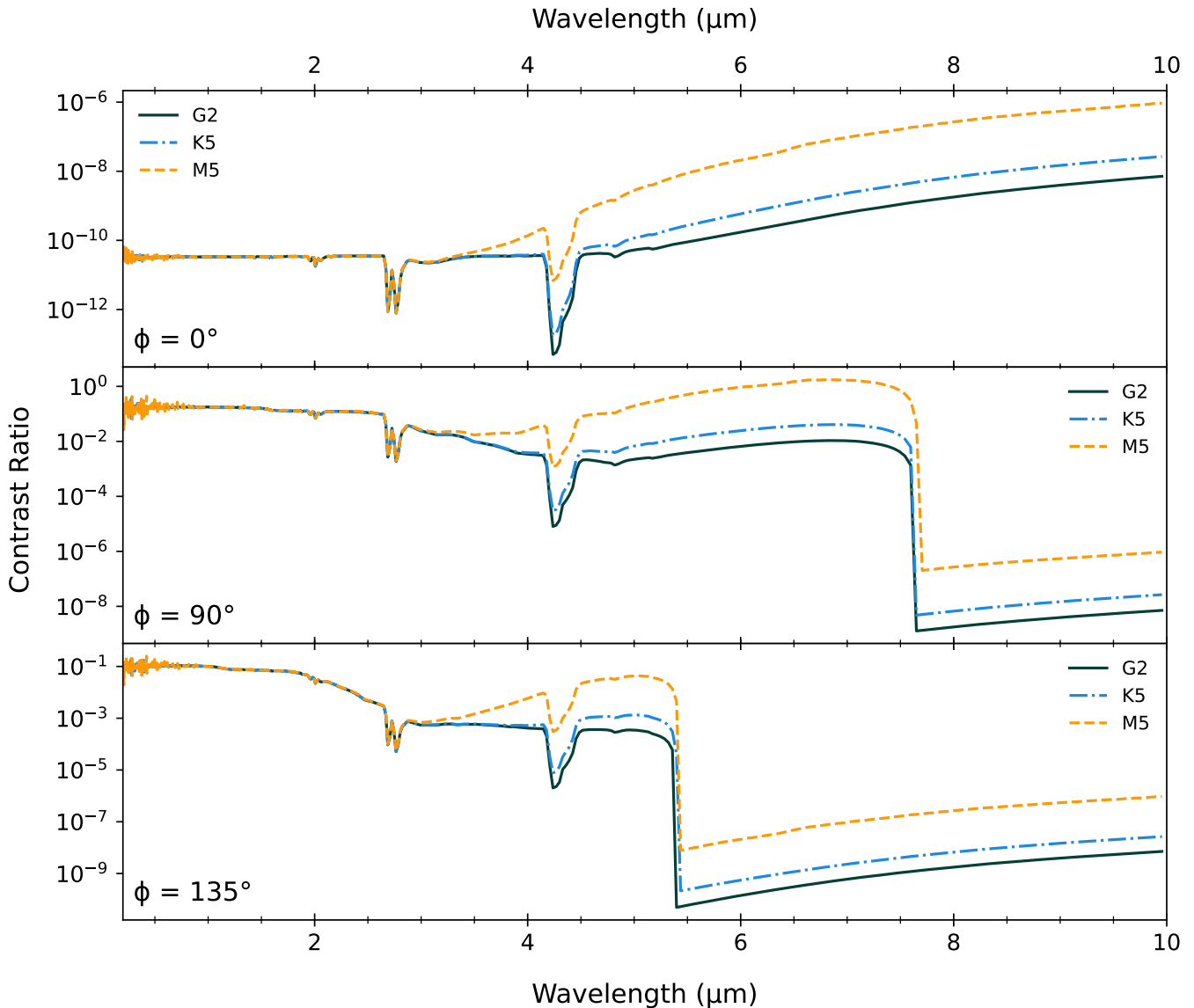


Figure 5. Reflectance spectra for a Mars analog in an edge-on orbit around G2 dwarf, K5 dwarf, and M5 host stars located at a distance of 10 pcs. The top, middle, and bottom panels correspond to planetary phase angles of 0° , 90° , and 135° , respectively.

is particularly constraining for sub-Earth masses (Joshi et al. 1997; Heng & Kopparla 2012; Wordsworth 2015).

Incident flux, spectral energy distribution, and orbital forcing all contribute to a planet’s ability to host surface liquid water. Particularly for small planets, secularly maintained eccentricity in compact systems can raise the orbit-averaged instellation and produce sustained tidal heating that either prolongs volcanism and degassing or forces runaway volatile loss and interior desiccation (Jackson et al. 2008; Kane & Gelino 2012b; Barnes et al. 2013; Van Laerhoven et al. 2014; Way & Georgakarakos 2017; Kane et al. 2021a). System architecture further modulates habitability by setting im-

pact fluxes and volatile delivery (e.g., the presence and spacing of giant planets), by locking planets into resonant chains that maintain eccentricity and tides, and by altering long-term obliquity stability (Raymond & Izidoro 2017; Turbet et al. 2018; Kane & Wittenmyer 2024; Kane & Miles 2025). Regarding the incident flux, updated radiative-convective models place the classical main-sequence HZ for Sun-like stars at incident flux $F_p/F_\oplus \sim 0.35\text{--}1.1$, but the effective outer edge for Mars-size planets is closer to the star because (i) CO_2 condenses more readily, and (ii) heat transport is less effective in thin atmospheres (Kopparapu et al. 2013, 2014; Wordsworth 2015). Conversely, transient green-

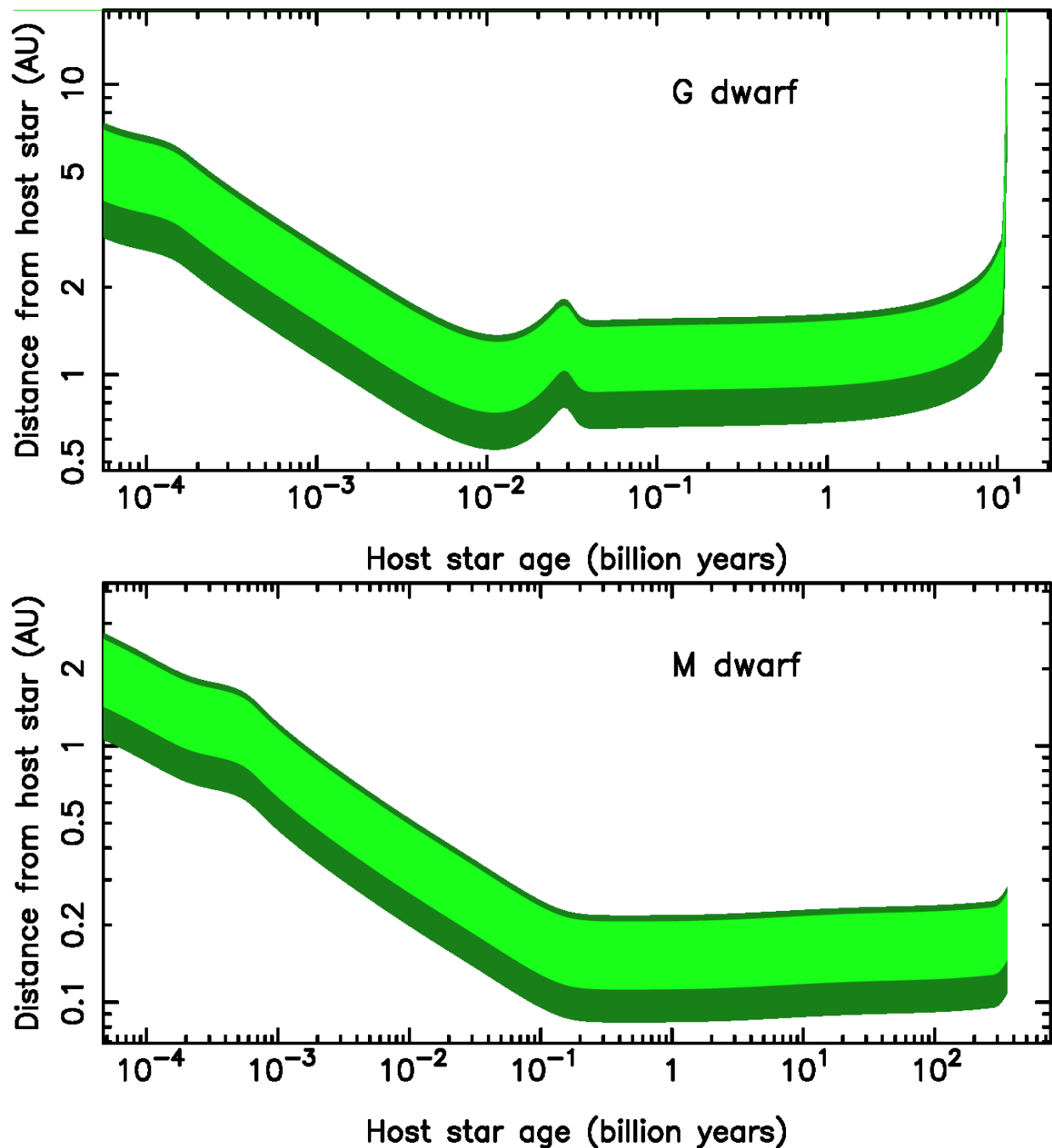


Figure 6. Evolution of the HZ before and during the main sequence for an G dwarf (top) and M-dwarf (bottom). The extent of the HZ is shown in green, where light green is the conservative HZ and dark green is the optimistic extension to the HZ.

house episodes (e.g., volcanic CO_2+H_2) can widen the viable window if outgassing sustains \gtrsim bar-level inventories (Ramirez & Kaltenegger 2017). Host-star spectral type also matters through the XUV/particle environment that sculpts escape and through the near-IR weighting of the stellar spectrum, which enhances H_2O and CO_2 absorption for late-type stars, modifying HZ

limits and the threshold for atmospheric collapse (Kopparapu et al. 2014; Turbet et al. 2016).

Shown in Figure 6 are examples of the HZ evolution for a G dwarf (top panel) and M-dwarf (bottom panel). The stellar properties and evolutionary tracks were calculated using the MESA Isochrones & Stellar Tracks (MIST) Paxton et al. (2011, 2013, 2015); Choi et al. (2016); Dotter (2016); Paxton et al. (2018, 2019). A

solar metallicity was assumed for both stars, and stellar masses of $0.3 M_{\odot}$ and $1.0 M_{\odot}$ were used for the M-dwarf and G dwarf, respectively. The conservative HZ (CHZ) is bounded by calculated limits of runaway greenhouse and maximum greenhouse transitions, and the optimistic HZ (OHZ) boundaries are determined via empirical evidence of past surface liquid water on the surfaces of Venus and Mars (Kopparapu et al. 2013; Kane et al. 2016). The CHZ is shown as light green in Figure 6, and the OHZ extension to the HZ is shown as dark green. To calculate the HZ boundaries, we adopted the $0.1 M_{\oplus}$ coefficients provided by (Kopparapu et al. 2014), whereby the inner edge of the CHZ moves outward due to an expected increased atmospheric H_2O column depth. The timescales and distances shown in Figure 6 demonstrate the extent to which the HZ evolution changes between G and M stars on the main sequence, particular the relative length of the pre-main sequence phase, which is considerably longer for M stars. Although the width of the HZ for M stars is quite narrow (~ 0.1 – 0.2 AU), it remains stable for many billions of years. However, the risk remains that the proximity of the Mars-mass planet to an extended period of increased stellar activity may result in a complete loss of atmosphere (see Section 2.3).

In summary, Mars-mass exoplanets are most likely to enjoy clement surface conditions early, when outgassing peaks, and later only if supplied by long-lived internal heat sources, tidal dissipation, or episodic volatile delivery. Long-term habitability is favored around quieter K/G stars at moderate incident flux, low-to-moderate eccentricity, and in architectures that neither overstimulate tides nor starve the planet of volatiles. By contrast, close-in M-dwarf planets require unusually robust volatile inventories, vigorous and persistent degassing, and/or magnetic and atmospheric protection to survive the pre-main-sequence and space-weather gauntlet (Luger & Barnes 2015; Airapetian et al. 2017; Noack et al. 2017).

6. DISCUSSION

6.1. *Lessons for Interpreting Rocky Exoplanets*

Studying Mars provides numerous lessons that translate directly into the interpretation of rocky exoplanet data. Regarding escape-driven desiccation and abiotic O_2 , long-term H escape from H_2O can leave O_2/O_3 -rich atmospheres without the need to invoke biological processes. However, it is important to note that coupled H and O escape may prevent significant O_2 accumulation in the atmosphere (McElroy 1972; Jakosky et al. 2018), and thus the degree to which abiotic O_2 can build up depends on the balance between production and loss

channels. Mars further constrains rates and controlling physics across dust seasons, informing false-positive assessments around M-dwarfs (Heavens et al. 2018). Mars provides empirical tests of general circulation models (GCMs) and analytic criteria for CO_2 freeze-out, and these results inform models of tidally locked exoplanets in/near the HZ, where atmospheric mass and heat transport determine survivability (Wordsworth 2015), though caution is warranted when extrapolating GCMs validated under present-day Martian conditions to dynamically distinct regimes where boundary conditions and processes may differ substantially. The noble-gas and hydrogen isotope fractionation under known escape regimes calibrate how we read future high-precision spectra of small exoplanet atmospheres (Mahaffy et al. 2013). Mars also informs the potential for habitable windows in the absence of plate tectonics. Sedimentary facies at Gale/Jezero demonstrate that long-lived surface waters can exist transiently, even as a planet trends toward aridity—guiding expectations for temporal habitability on small exoplanets (Grotzinger et al. 2014).

6.2. *Recommended Search Program for Mars Analogs*

As detailed in Section 4, the detection of Mars analogs is a challenging task as the required sensitivity lies at the edge or beyond for the majority of exoplanet detection techniques. The most promising near-term discovery pathways include transit+TTV observations of compact systems around late M-dwarfs (Gillon et al. 2017; Agol et al. 2021) and the Roman microlensing survey of bulge fields (Penny et al. 2019). The long-term goals are to characterize the atmospheres of low-mass planets, empirically modeling their evolutions from early degassing stages through to later more tenuous states. Validation of retrieval techniques based on disk-integrated spectra of Solar System planets have provided invaluable insight into the requirements of achieving such goals (Kane et al. 2021b; Robinson & Salvador 2023). Combining thermal-infrared observations of the nearest Mars-analog exoplanet candidates (Wolfe & Robinson 2024), reflected-light imaging with HWO-class facilities, and mid-infrared interferometry with concepts such as LIFE (Quanz et al. 2022) will ultimately quantify the occurrence rate and atmospheric properties of true Mars analogs, although confirmation of their exact mass, composition, and habitability will remain observationally demanding.

6.3. *Priority Topics for Mars Exploration*

In the most recent planetary science Decadal Survey, *Origins, Worlds, and Life*¹, Mars features heavily both as a worthy Solar System target in its own right and as a basis for better understanding rocky exoplanets. Through a series of Strategic Research (SR) activities within 12 Priority Science Questions, key Solar System science topics can be addressed by studying myriad aspects of the Mars system. For example, in Priority Question 3, "Origin of Earth and Inner Solar System Bodies", SR 3.4 includes the objective to "Determine the formation time of Mars through isotopic analyses of diverse Martian samples," something that could be achieved through, for example, the return to Earth of samples from the Red Planet. Similarly, in Priority Question 6, "Solid Body Atmospheres, Exospheres, Magnetospheres, and Climate Evolution" there are two SRs specific to understanding the atmospheric evolution of Mars. One, SR 6.1, states "Constrain the earliest stages of atmospheric evolution on Venus, Mars, and Titan by measuring noble gas abundances and isotopic fractionation to sufficient precision to quantify their minor isotopes." For the second, SR 6.2, the objective is to "Determine how and why Mars's climate has changed over orbital timescales by performing radar and spectroscopic mapping of the polar layered terrain and by making in situ measurements of their structure and composition (thickness of layers, dust content, and isotope ratios) and their local meteorology (including volatile and dust fluxes)."

These are specific tasks that can be carried out at Mars or on Earth with Mars samples, and are directly in service of better understanding the modern state of the planet and how it got that way. In that same Priority Question, however, SR 6.6 reads "Investigate the microphysical parameters that influence the formation of clouds in planetary atmospheres (primarily... Mars...) by determining the distribution, nature, and abundance of clouds and the composition and particle size of the droplets comprising them and cloud condensation nuclei around which they form." This investigation would have direct bearing on efforts to characterize rocky-exoplanet atmospheres in terms of distinguishing potential cloud spectral signatures from that of the bulk atmosphere.

Moreover, *Origins, Worlds, and Life* also includes an exoplanet-focused chapter, written explicitly with the goal of using that understanding of Mars to further our (remote) exploration of terrestrial exoplanets. For instance, in the Priority Question 12, "Exoplanets", SR 12.10 is to "Determine the properties of the atmospheres

of terrestrial planets (i.e., ... Mars) that would be observable on exoplanets to build a foundation for atmospheric characterization of analogue exoplanets through coordinating in situ/remote sensing measurements and theoretical studies of wind velocities, radiative balance, cloud dynamics, and atmospheric compositing as function of orbital phase, local time, and solar conditions." SR 12.10 states "Improve exoplanet habitability predictions for cold, low-mass planets by determining the key factors that made Mars habitable 3–4 Ga, via a combination of in situ geological and atmospheric analysis and sample return, orbital observations, and climate modeling." And in SR 12.11, the decadal survey advises "Study methods to discriminate past and present false positive biosignatures on Solar System bodies (e.g., abiotic O₂ on... Mars) from true biosignatures to inform false positive discrimination methods for exoplanets through in situ, remote sensing, theoretical/modeling studies, analog field research, and laboratory studies that characterize remotely observable properties of these features."

Together, these activities if implemented would advance not only our understanding of Mars' past and present states but would more firmly place it as a foundation for how we identify and interpret Mars-analog exoplanet features and properties.

7. CONCLUSIONS

Mars occupies an important position in comparative planetology, since it is both a geologically rich world with a documented history of surface habitability, and a representative example of how small rocky planets can evolve toward atmospheric loss and climatic decline. Through examination of its various properties, such as formation history, orbital evolution, interior cooling, and atmospheric escape, we have shown that Mars provides a physically grounded framework for interpreting sub-Earth exoplanets. The geological and atmospheric evolution of Mars underscores that habitability is not a static property, but is a time-dependent outcome governed by competing processes. Early volcanism and volatile release likely supported a thicker atmosphere and surface liquid water, yet declining interior heat flow, cessation of dynamo activity, and sustained atmospheric escape gradually reduced surface pressure and limited climate stability. These coupled processes can define a pathway that may be common for Mars-mass planets. In this context, Mars represents the edge of the habitable regime, being large enough to host transiently clement conditions, but small enough that atmospheric retention and replenishment and long-term climate regulation are not guaranteed.

¹ <https://doi.org/10.17226/26522>

Our discussion of exoplanet demographics have shown that, while terrestrial-size planets are abundant, confirmed Mars-mass planets with well-constrained masses and radii remain relatively rare, largely due to detection shortcomings. Transit and RV surveys favor larger or more strongly irradiated planets, and the smallest rocky bodies challenge current sensitivity limits. The coming Roman microlensing surveys offer a particularly promising avenue for probing the true frequency of Mars analogs. Direct imaging and thermal emission studies, particularly with next-generation facilities, will ultimately determine whether such planets commonly retain thin CO₂ atmospheres, undergo desiccation, or exhibit transient volatile cycles.

Ultimately, the convergence of Solar System exploration and exoplanet characterization provides a powerful strategy for understanding small rocky worlds. Mars missions will continue to measure atmospheric escape rates, volatile inventories, and climate feedbacks with a level of detail unattainable for exoplanets, while exoplanet surveys contextualize Mars within a broader statistical population. Together, these complementary approaches identify key science priorities, including under-

standing the mass threshold for sustained geologic activity, quantifying atmospheric survival as a function of stellar environment, assessing the stability of thin CO₂ atmospheres, and refining observational techniques capable of detecting sub-Earth planets. Within this framework, Mars provides a fundamental benchmark for evaluating the diversity, evolution, and potential habitability of rocky planets throughout the Galaxy.

ACKNOWLEDGEMENTS

The research described in this paper has benefited from useful conversations with Brian Jackson. The authors also acknowledge the valuable feedback provided by Bruce Jakosky and an additional anonymous reviewer. This research has made use of the Habitable Zone Gallery at hzgl.org. The results reported herein benefited from collaborations and/or information exchange within NASA's Nexus for Exoplanet System Science (NExSS) research coordination network sponsored by NASA's Science Mission Directorate.

Software: Planetary Spectrum Generator (PSG; [Vilanova et al. 2018](#))

REFERENCES

- Acuna, M. H., Connerney, J. E. P., Ness, N. F., et al. 1999, *Science*, 284, 790, doi: [10.1126/science.284.5415.790](https://doi.org/10.1126/science.284.5415.790)
- Adams, A. D., Colose, C., Merrelli, A., Turnbull, M., & Kane, S. R. 2025, *ApJ*, 981, 98, doi: [10.3847/1538-4357/ada3c8](https://doi.org/10.3847/1538-4357/ada3c8)
- Agol, E., Dorn, C., Grimm, S. L., et al. 2021, *PSJ*, 2, 1, doi: [10.3847/PSJ/abd022](https://doi.org/10.3847/PSJ/abd022)
- Aigrain, S., Favata, F., & Gilmore, G. 2004, *A&A*, 414, 1139, doi: [10.1051/0004-6361:20034039](https://doi.org/10.1051/0004-6361:20034039)
- Airapetian, V. S., Glocer, A., Khazanov, G. V., et al. 2017, *ApJL*, 836, L3, doi: [10.3847/2041-8213/836/1/L3](https://doi.org/10.3847/2041-8213/836/1/L3)
- Albrow, M. D., An, J., Beaulieu, J. P., et al. 2001, *ApJL*, 556, L113, doi: [10.1086/323141](https://doi.org/10.1086/323141)
- Apai, D., Barnes, R., Murphy, M. M., et al. 2025, *PSJ*, 6, 165, doi: [10.3847/PSJ/addda8](https://doi.org/10.3847/PSJ/addda8)
- Barclay, T., Rowe, J. F., Lissauer, J. J., et al. 2013, *Nature*, 494, 452, doi: [10.1038/nature11914](https://doi.org/10.1038/nature11914)
- Barnes, R., Mullins, K., Goldblatt, C., et al. 2013, *Astrobiology*, 13, 225, doi: [10.1089/ast.2012.0851](https://doi.org/10.1089/ast.2012.0851)
- Basak, A., & Nandy, D. 2021, *MNRAS*, 502, 3569, doi: [10.1093/mnras/stab225](https://doi.org/10.1093/mnras/stab225)
- Berger, T. A., Huber, D., Gaidos, E., & van Saders, J. L. 2018, *ApJ*, 866, 99, doi: [10.3847/1538-4357/aada83](https://doi.org/10.3847/1538-4357/aada83)
- Bibring, J.-P., Langevin, Y., Mustard, J. F., et al. 2006, *Science*, 312, 400, doi: [10.1126/science.1122659](https://doi.org/10.1126/science.1122659)
- Boettner, C., Viswanathan, A., & Dayal, P. 2024, *A&A*, 692, A150, doi: [10.1051/0004-6361/202451537](https://doi.org/10.1051/0004-6361/202451537)
- Bolmont, E., Selsis, F., Owen, J. E., et al. 2017, *MNRAS*, 464, 3728, doi: [10.1093/mnras/stw2578](https://doi.org/10.1093/mnras/stw2578)
- Borucki, W. J. 2016, *Reports on Progress in Physics*, 79, 036901, doi: [10.1088/0034-4885/79/3/036901](https://doi.org/10.1088/0034-4885/79/3/036901)
- Borucki, W. J., Koch, D., Basri, G., et al. 2010, *Science*, 327, 977, doi: [10.1126/science.1185402](https://doi.org/10.1126/science.1185402)
- Brady, M. T., & Bean, J. L. 2022, *AJ*, 163, 255, doi: [10.3847/1538-3881/ac64a0](https://doi.org/10.3847/1538-3881/ac64a0)
- Brain, D. A., Bagenal, F., Ma, Y. J., Nilsson, H., & Stenberg Wieser, G. 2016, *Journal of Geophysical Research (Planets)*, 121, 2364, doi: [10.1002/2016JE005162](https://doi.org/10.1002/2016JE005162)
- Brain, D. A., Leblanc, F., Luhmann, J. G., Moore, T. E., & Tian, F. 2013, in *Comparative Climatology of Terrestrial Planets*, ed. S. J. Mackwell, A. A. Simon-Miller, J. W. Harder, & M. A. Bullock (University of Arizona Press), 487–503, doi: [10.2458/azu_uapress.9780816530595-ch020](https://doi.org/10.2458/azu_uapress.9780816530595-ch020)
- Brain, D. A., Cohen, O., Cravens, T. E., et al. 2026, *arXiv e-prints*, arXiv:2603.11561, doi: [10.48550/arXiv.2603.11561](https://doi.org/10.48550/arXiv.2603.11561)
- Brandt, T. D. 2018, *ApJS*, 239, 31, doi: [10.3847/1538-4365/aaec06](https://doi.org/10.3847/1538-4365/aaec06)
- . 2021, *ApJS*, 254, 42, doi: [10.3847/1538-4365/abf93c](https://doi.org/10.3847/1538-4365/abf93c)

- Butler, R. P., Wright, J. T., Marcy, G. W., et al. 2006, *ApJ*, 646, 505, doi: [10.1086/504701](https://doi.org/10.1086/504701)
- Byrne, P. K. 2020, *Nature Astronomy*, 4, 321, doi: [10.1038/s41550-019-0944-3](https://doi.org/10.1038/s41550-019-0944-3)
- Cañas, C. I., Mahadevan, S., Cochran, W. D., et al. 2022, *AJ*, 163, 3, doi: [10.3847/1538-3881/ac3088](https://doi.org/10.3847/1538-3881/ac3088)
- Cale, B. L., Reefe, M., Plavchan, P., et al. 2021, *AJ*, 162, 295, doi: [10.3847/1538-3881/ac2c80](https://doi.org/10.3847/1538-3881/ac2c80)
- Campante, T. L., Barclay, T., Swift, J. J., et al. 2015, *ApJ*, 799, 170, doi: [10.1088/0004-637X/799/2/170](https://doi.org/10.1088/0004-637X/799/2/170)
- Cassan, A., Kubas, D., Beaulieu, J.-P., et al. 2012, *Nature*, 481, 167, doi: [10.1038/nature10684](https://doi.org/10.1038/nature10684)
- Chaffin, M. S., Chaufray, J.-Y., Stewart, I., et al. 2014, *Geophys. Res. Lett.*, 41, 314, doi: [10.1002/2013GL058578](https://doi.org/10.1002/2013GL058578)
- Chaffin, M. S., Kass, D. M., Aoki, S., et al. 2021, *Nature Astronomy*, 5, 1036, doi: [10.1038/s41550-021-01425-w](https://doi.org/10.1038/s41550-021-01425-w)
- Chassefière, E., & Leblanc, F. 2004, *Planet. Space Sci.*, 52, 1039, doi: [10.1016/j.pss.2004.07.002](https://doi.org/10.1016/j.pss.2004.07.002)
- Choi, J., Dotter, A., Conroy, C., et al. 2016, *ApJ*, 823, 102, doi: [10.3847/0004-637X/823/2/102](https://doi.org/10.3847/0004-637X/823/2/102)
- Chomez, A., Delorme, P., Lagrange, A.-M., et al. 2025, *A&A*, 697, A99, doi: [10.1051/0004-6361/202451751](https://doi.org/10.1051/0004-6361/202451751)
- Christiansen, J. L., McElroy, D. L., Harbut, M., et al. 2025, *PSJ*, 6, 186, doi: [10.3847/PSJ/ade3c2](https://doi.org/10.3847/PSJ/ade3c2)
- Ciardi, D. R., von Braun, K., Bryden, G., et al. 2011, *AJ*, 141, 108, doi: [10.1088/0004-6256/141/4/108](https://doi.org/10.1088/0004-6256/141/4/108)
- Cockell, C. S. 2014, *Astrobiology*, 14, 182, doi: [10.1089/ast.2013.1106](https://doi.org/10.1089/ast.2013.1106)
- Connerney, J. E. P., Acuna, M. H., Wasilewski, P. J., et al. 1999, *Science*, 284, 794, doi: [10.1126/science.284.5415.794](https://doi.org/10.1126/science.284.5415.794)
- Damiano, M., Hu, R., Barclay, T., et al. 2022, *AJ*, 164, 225, doi: [10.3847/1538-3881/ac9472](https://doi.org/10.3847/1538-3881/ac9472)
- Dauphas, N., & Pourmand, A. 2011, *Nature*, 473, 489, doi: [10.1038/nature10077](https://doi.org/10.1038/nature10077)
- de Laverny, P., Ligi, R., Crida, A., Recio-Blanco, A., & Palicio, P. A. 2025, *A&A*, 699, A100, doi: [10.1051/0004-6361/202554739](https://doi.org/10.1051/0004-6361/202554739)
- Demangeon, O. D. S., Zapatero Osorio, M. R., Alibert, Y., et al. 2021, *A&A*, 653, A41, doi: [10.1051/0004-6361/202140728](https://doi.org/10.1051/0004-6361/202140728)
- Dong, C., Jin, M., Lingam, M., et al. 2018a, *Proceedings of the National Academy of Science*, 115, 260, doi: [10.1073/pnas.1708010115](https://doi.org/10.1073/pnas.1708010115)
- Dong, C., Lee, Y., Ma, Y., et al. 2018b, *ApJL*, 859, L14, doi: [10.3847/2041-8213/aac489](https://doi.org/10.3847/2041-8213/aac489)
- Dorn, C., Khan, A., Heng, K., et al. 2015, *A&A*, 577, A83, doi: [10.1051/0004-6361/201424915](https://doi.org/10.1051/0004-6361/201424915)
- Dotter, A. 2016, *ApJS*, 222, 8, doi: [10.3847/0067-0049/222/1/8](https://doi.org/10.3847/0067-0049/222/1/8)
- Dressing, C. D., & Charbonneau, D. 2015, *ApJ*, 807, 45, doi: [10.1088/0004-637X/807/1/45](https://doi.org/10.1088/0004-637X/807/1/45)
- Driscoll, P., & Bercovici, D. 2013, *Icarus*, 226, 1447, doi: [10.1016/j.icarus.2013.07.025](https://doi.org/10.1016/j.icarus.2013.07.025)
- Ehlmann, B. L., & Edwards, C. S. 2014, *Annual Review of Earth and Planetary Sciences*, 42, 291, doi: [10.1146/annurev-earth-060313-055024](https://doi.org/10.1146/annurev-earth-060313-055024)
- Ehlmann, B. L., Mustard, J. F., & Murchie, S. L. 2010, *Geophys. Res. Lett.*, 37, L06201, doi: [10.1029/2010GL042596](https://doi.org/10.1029/2010GL042596)
- Ehlmann, B. L., Mustard, J. F., Murchie, S. L., et al. 2011, *Nature*, 479, 53, doi: [10.1038/nature10582](https://doi.org/10.1038/nature10582)
- Ehlmann, B. L., Mustard, J. F., Swayze, G. A., et al. 2009, *Journal of Geophysical Research (Planets)*, 114, E00D08, doi: [10.1029/2009JE003339](https://doi.org/10.1029/2009JE003339)
- Elkins-Tanton, L. T. 2008, *Earth and Planetary Science Letters*, 271, 181, doi: [10.1016/j.epsl.2008.03.062](https://doi.org/10.1016/j.epsl.2008.03.062)
- Fatheddin, H., & Sajadian, S. 2023, *AJ*, 166, 140, doi: [10.3847/1538-3881/aced8b](https://doi.org/10.3847/1538-3881/aced8b)
- Fetherolf, T., Pepper, J., Simpson, E., et al. 2023, *ApJS*, 268, 4, doi: [10.3847/1538-4365/acdee5](https://doi.org/10.3847/1538-4365/acdee5)
- Fischer, D. A., Anglada-Escude, G., Arriagada, P., et al. 2016, *PASP*, 128, 066001, doi: [10.1088/1538-3873/128/964/066001](https://doi.org/10.1088/1538-3873/128/964/066001)
- Foley, B. J., & Smye, A. J. 2018, *Astrobiology*, 18, 873, doi: [10.1089/ast.2017.1695](https://doi.org/10.1089/ast.2017.1695)
- Ford, E. B. 2014, *Proceedings of the National Academy of Science*, 111, 12616, doi: [10.1073/pnas.1304219111](https://doi.org/10.1073/pnas.1304219111)
- Forget, F., Haberle, R. M., Montmessin, F., Levrard, B., & Head, J. W. 2006, *Science*, 311, 368, doi: [10.1126/science.1120335](https://doi.org/10.1126/science.1120335)
- Fressin, F., Torres, G., Charbonneau, D., et al. 2013, *ApJ*, 766, 81, doi: [10.1088/0004-637X/766/2/81](https://doi.org/10.1088/0004-637X/766/2/81)
- Fujii, Y., Angerhausen, D., Deitrick, R., et al. 2018, *Astrobiology*, 18, 739, doi: [10.1089/ast.2017.1733](https://doi.org/10.1089/ast.2017.1733)
- Fulton, B. J., & Petigura, E. A. 2018, *AJ*, 156, 264, doi: [10.3847/1538-3881/aae828](https://doi.org/10.3847/1538-3881/aae828)
- Gaia Collaboration, Brown, A. G. A., Vallenari, A., et al. 2021, *A&A*, 649, A1, doi: [10.1051/0004-6361/202039657](https://doi.org/10.1051/0004-6361/202039657)
- García Muñoz, A., & Cabrera, J. 2018, *MNRAS*, 473, 1801, doi: [10.1093/mnras/stx2428](https://doi.org/10.1093/mnras/stx2428)
- Gaudi, B. S. 2012, *ARA&A*, 50, 411, doi: [10.1146/annurev-astro-081811-125518](https://doi.org/10.1146/annurev-astro-081811-125518)
- Gibson, S. R., Howard, A. W., Marcy, G. W., et al. 2016, in *Society of Photo-Optical Instrumentation Engineers (SPIE) Conference Series*, Vol. 9908, *Ground-based and Airborne Instrumentation for Astronomy VI*, ed. C. J. Evans, L. Simard, & H. Takami, 990870, doi: [10.1117/12.2233334](https://doi.org/10.1117/12.2233334)

- Gillon, M., Triaud, A. H. M. J., Demory, B.-O., et al. 2017, *Nature*, 542, 456, doi: [10.1038/nature21360](https://doi.org/10.1038/nature21360)
- Glidden, A., Ranjan, S., Seager, S., et al. 2025, *ApJL*, 990, L53, doi: [10.3847/2041-8213/adf62e](https://doi.org/10.3847/2041-8213/adf62e)
- Gould, A., & Loeb, A. 1992, *ApJ*, 396, 104, doi: [10.1086/171700](https://doi.org/10.1086/171700)
- Greene, T. P., Bell, T. J., Ducrot, E., et al. 2023, *Nature*, 618, 39, doi: [10.1038/s41586-023-05951-7](https://doi.org/10.1038/s41586-023-05951-7)
- Grimm, S. L., Demory, B.-O., Gillon, M., et al. 2018, *A&A*, 613, A68, doi: [10.1051/0004-6361/201732233](https://doi.org/10.1051/0004-6361/201732233)
- Grott, M., Breuer, D., & Laneville, M. 2011, *Earth and Planetary Science Letters*, 307, 135, doi: [10.1016/j.epsl.2011.04.040](https://doi.org/10.1016/j.epsl.2011.04.040)
- Grotzinger, J. P. 2014, *Science*, 343, 386, doi: [10.1126/science.1249944](https://doi.org/10.1126/science.1249944)
- Grotzinger, J. P., Sumner, D. Y., Kah, L. C., et al. 2014, *Science*, 343, 1242777, doi: [10.1126/science.1242777](https://doi.org/10.1126/science.1242777)
- Gunell, H., Maggiolo, R., Nilsson, H., et al. 2018, *A&A*, 614, L3, doi: [10.1051/0004-6361/201832934](https://doi.org/10.1051/0004-6361/201832934)
- Guzewich, S. D., Lustig-Yaeger, J., Davis, C. E., et al. 2020, *ApJ*, 893, 140, doi: [10.3847/1538-4357/ab83ec](https://doi.org/10.3847/1538-4357/ab83ec)
- Hansen, B. M. S. 2009, *ApJ*, 703, 1131, doi: [10.1088/0004-637X/703/1/1131](https://doi.org/10.1088/0004-637X/703/1/1131)
- Harada, C. K., Dressing, C. D., Kane, S. R., & Ardestani, B. A. 2024, *ApJS*, 272, 30, doi: [10.3847/1538-4365/ad3e81](https://doi.org/10.3847/1538-4365/ad3e81)
- Heavens, N. G., Kleinböhl, A., Chaffin, M. S., et al. 2018, *Nature Astronomy*, 2, 126, doi: [10.1038/s41550-017-0353-4](https://doi.org/10.1038/s41550-017-0353-4)
- Heller, R., Harre, J.-V., & Samadi, R. 2022, *A&A*, 665, A11, doi: [10.1051/0004-6361/202141640](https://doi.org/10.1051/0004-6361/202141640)
- Heng, K., & Kopparla, P. 2012, *ApJ*, 754, 60, doi: [10.1088/0004-637X/754/1/60](https://doi.org/10.1088/0004-637X/754/1/60)
- Hill, M. L., Bott, K., Dalba, P. A., et al. 2023, *AJ*, 165, 34, doi: [10.3847/1538-3881/aca1c0](https://doi.org/10.3847/1538-3881/aca1c0)
- Hill, M. L., Kane, S. R., Foley, B. J., & Schaefer, L. K. 2026, arXiv e-prints, arXiv:2605.00170. <https://arxiv.org/abs/2605.00170>
- Hill, M. L., Kane, S. R., Seperuelo Duarte, E., et al. 2018, *ApJ*, 860, 67, doi: [10.3847/1538-4357/aac384](https://doi.org/10.3847/1538-4357/aac384)
- Horner, J., Kane, S. R., Marshall, J. P., et al. 2020, *PASP*, 132, 102001, doi: [10.1088/1538-3873/ab8eb9](https://doi.org/10.1088/1538-3873/ab8eb9)
- Howard, A. W., Marcy, G. W., Johnson, J. A., et al. 2010, *Science*, 330, 653, doi: [10.1126/science.1194854](https://doi.org/10.1126/science.1194854)
- Hu, R., Kass, D. M., Ehlmann, B. L., & Yung, Y. L. 2015, *Nature Communications*, 6, 10003, doi: [10.1038/ncomms10003](https://doi.org/10.1038/ncomms10003)
- Hurowitz, J. A., Grotzinger, J. P., Fischer, W. W., et al. 2017, *Science*, 356, aah6849, doi: [10.1126/science.aah6849](https://doi.org/10.1126/science.aah6849)
- Jackson, B., Greenberg, R., & Barnes, R. 2008, *ApJ*, 678, 1396, doi: [10.1086/529187](https://doi.org/10.1086/529187)
- Jakosky, B. M. 2021, *Annual Review of Earth and Planetary Sciences*, 49, doi: [10.1146/annurev-earth-062420-052845](https://doi.org/10.1146/annurev-earth-062420-052845)
- Jakosky, B. M., & Byrne, P. K. 2025, *Journal of Geophysical Research (Planets)*, 130, e2024JE008882, doi: [10.1029/2024JE008882](https://doi.org/10.1029/2024JE008882)
- Jakosky, B. M., Henderson, B. G., & Mellon, M. T. 1995, *J. Geophys. Res.*, 100, 1579, doi: [10.1029/94JE02801](https://doi.org/10.1029/94JE02801)
- Jakosky, B. M., Pepin, R. O., Johnson, R. E., & Fox, J. L. 1994, *Icarus*, 111, 271, doi: [10.1006/icar.1994.1145](https://doi.org/10.1006/icar.1994.1145)
- Jakosky, B. M., & Phillips, R. J. 2001, *Nature*, 412, 237, doi: [10.1038/35084184](https://doi.org/10.1038/35084184)
- Jakosky, B. M., Slipski, M., Benna, M., et al. 2017, *Science*, 355, 1408, doi: [10.1126/science.aai7721](https://doi.org/10.1126/science.aai7721)
- Jakosky, B. M., & Treiman, A. H. 2023, *Icarus*, 402, 115627, doi: [10.1016/j.icarus.2023.115627](https://doi.org/10.1016/j.icarus.2023.115627)
- Jakosky, B. M., Grebowsky, J. M., Luhmann, J. G., et al. 2015, *Science*, 350, 0210, doi: [10.1126/science.aad0210](https://doi.org/10.1126/science.aad0210)
- Jakosky, B. M., Brain, D., Chaffin, M., et al. 2018, *Icarus*, 315, 146, doi: [10.1016/j.icarus.2018.05.030](https://doi.org/10.1016/j.icarus.2018.05.030)
- Joiret, S., Morbidelli, A., de Sousa Ribeiro, R., Avice, G., & Sossi, P. 2025, *Earth and Planetary Science Letters*, 671, 119625, doi: [10.1016/j.epsl.2025.119625](https://doi.org/10.1016/j.epsl.2025.119625)
- Jontof-Hutter, D., Rowe, J. F., Lissauer, J. J., Fabrycky, D. C., & Ford, E. B. 2015, *Nature*, 522, 321, doi: [10.1038/nature14494](https://doi.org/10.1038/nature14494)
- Joshi, M. M., Haberle, R. M., & Reynolds, R. T. 1997, *Icarus*, 129, 450, doi: [10.1006/icar.1997.5793](https://doi.org/10.1006/icar.1997.5793)
- Jurgenson, C., Fischer, D., McCracken, T., et al. 2016, in *Society of Photo-Optical Instrumentation Engineers (SPIE) Conference Series*, Vol. 9908, Ground-based and Airborne Instrumentation for Astronomy VI, ed. C. J. Evans, L. Simard, & H. Takami, 99086T, doi: [10.1117/12.2233002](https://doi.org/10.1117/12.2233002)
- Kane, S. R. 2011, *Icarus*, 214, 327, doi: [10.1016/j.icarus.2011.04.023](https://doi.org/10.1016/j.icarus.2011.04.023)
- Kane, S. R., & Gelino, D. M. 2010, *ApJ*, 724, 818, doi: [10.1088/0004-637X/724/1/818](https://doi.org/10.1088/0004-637X/724/1/818)
- . 2011a, *ApJ*, 729, 74, doi: [10.1088/0004-637X/729/1/74](https://doi.org/10.1088/0004-637X/729/1/74)
- . 2011b, *ApJ*, 741, 52, doi: [10.1088/0004-637X/741/1/52](https://doi.org/10.1088/0004-637X/741/1/52)
- . 2012a, *PASP*, 124, 323, doi: [10.1086/665271](https://doi.org/10.1086/665271)
- . 2012b, *Astrobiology*, 12, 940, doi: [10.1089/ast.2011.0798](https://doi.org/10.1089/ast.2011.0798)
- Kane, S. R., Li, Z., Turnbull, M. C., Dressing, C. D., & Harada, C. K. 2024, *AJ*, 168, 195, doi: [10.3847/1538-3881/ad6a50](https://doi.org/10.3847/1538-3881/ad6a50)
- Kane, S. R., Li, Z., Wolf, E. T., Ostberg, C., & Hill, M. L. 2021a, *AJ*, 161, 31, doi: [10.3847/1538-3881/abcbfd](https://doi.org/10.3847/1538-3881/abcbfd)

- Kane, S. R., & Miles, E. L. 2025, *AJ*, 170, 81, doi: [10.3847/1538-3881/ade305](https://doi.org/10.3847/1538-3881/ade305)
- Kane, S. R., Vervoort, P., & Horner, J. 2025, *PASP*, 137, 124402, doi: [10.1088/1538-3873/ae2800](https://doi.org/10.1088/1538-3873/ae2800)
- Kane, S. R., & von Braun, K. 2008, *ApJ*, 689, 492, doi: [10.1086/592381](https://doi.org/10.1086/592381)
- Kane, S. R., & Wittenmyer, R. A. 2024, *ApJL*, 962, L21, doi: [10.3847/2041-8213/ad2463](https://doi.org/10.3847/2041-8213/ad2463)
- Kane, S. R., Hill, M. L., Kasting, J. F., et al. 2016, *ApJ*, 830, 1, doi: [10.3847/0004-637X/830/1/1](https://doi.org/10.3847/0004-637X/830/1/1)
- Kane, S. R., Arney, G. N., Byrne, P. K., et al. 2021b, *Journal of Geophysical Research (Planets)*, 126, e06643, doi: [10.1002/jgre.v126.2](https://doi.org/10.1002/jgre.v126.2)
- Kane, S. R., Bean, J. L., Campante, T. L., et al. 2021c, *PASP*, 133, 014402, doi: [10.1088/1538-3873/abc610](https://doi.org/10.1088/1538-3873/abc610)
- Kasting, J. F. 1993, *Science*, 259, 920, doi: [10.1126/science.259.5097.920](https://doi.org/10.1126/science.259.5097.920)
- Kasting, J. F., Whitmire, D. P., & Reynolds, R. T. 1993, *Icarus*, 101, 108, doi: [10.1006/icar.1993.1010](https://doi.org/10.1006/icar.1993.1010)
- Kawashima, Y., & Rugheimer, S. 2019, *AJ*, 157, 213, doi: [10.3847/1538-3881/ab14e3](https://doi.org/10.3847/1538-3881/ab14e3)
- Khuller, A. R., & Clow, G. D. 2024, *Journal of Geophysical Research (Planets)*, 129, e2023JE008114, doi: [10.1029/2023JE008114](https://doi.org/10.1029/2023JE008114)
- Kiefer, F. 2019, *A&A*, 632, L9, doi: [10.1051/0004-6361/201936942](https://doi.org/10.1051/0004-6361/201936942)
- Kim, S.-L., Lee, C.-U., Park, B.-G., et al. 2016, *Journal of Korean Astronomical Society*, 49, 37, doi: [10.5303/JKAS.2016.49.1.37](https://doi.org/10.5303/JKAS.2016.49.1.37)
- Kite, E. S. 2019, *SSRv*, 215, 10, doi: [10.1007/s11214-018-0575-5](https://doi.org/10.1007/s11214-018-0575-5)
- Kopparapu, R. K., Ramirez, R. M., SchottelKotte, J., et al. 2014, *ApJ*, 787, L29, doi: [10.1088/2041-8205/787/2/L29](https://doi.org/10.1088/2041-8205/787/2/L29)
- Kopparapu, R. K., Ramirez, R., Kasting, J. F., et al. 2013, *ApJ*, 765, 131, doi: [10.1088/0004-637X/765/2/131](https://doi.org/10.1088/0004-637X/765/2/131)
- Krasnopolsky, V. A. 2006, *Icarus*, 185, 153, doi: [10.1016/j.icarus.2006.06.003](https://doi.org/10.1016/j.icarus.2006.06.003)
- Kreidberg, L., & Stevenson, K. B. 2025, *Proceedings of the National Academy of Science*, 122, e2416190122, doi: [10.1073/pnas.2416190122](https://doi.org/10.1073/pnas.2416190122)
- Lammer, H., Kasting, J. F., Chassefière, E., et al. 2008, *SSRv*, 139, 399, doi: [10.1007/s11214-008-9413-5](https://doi.org/10.1007/s11214-008-9413-5)
- Lammer, H., Chassefière, E., Karatekin, Ö., et al. 2013, *SSRv*, 174, 113, doi: [10.1007/s11214-012-9943-8](https://doi.org/10.1007/s11214-012-9943-8)
- Laskar, J., Correia, A. C. M., Gastineau, M., et al. 2004, *Icarus*, 170, 343, doi: [10.1016/j.icarus.2004.04.005](https://doi.org/10.1016/j.icarus.2004.04.005)
- Laskar, J., & Gastineau, M. 2009, *Nature*, 459, 817, doi: [10.1038/nature08096](https://doi.org/10.1038/nature08096)
- Laskar, J., Joutel, F., & Robutel, P. 1993, *Nature*, 361, 615, doi: [10.1038/361615a0](https://doi.org/10.1038/361615a0)
- Laskar, J., & Robutel, P. 1993, *Nature*, 361, 608, doi: [10.1038/361608a0](https://doi.org/10.1038/361608a0)
- Lefèvre, F., & Forget, F. 2009, *Nature*, 460, 720, doi: [10.1038/nature08228](https://doi.org/10.1038/nature08228)
- Lillis, R. J., Robbins, S., Manga, M., Halekas, J. S., & Frey, H. V. 2013, *Journal of Geophysical Research (Planets)*, 118, 1488, doi: [10.1002/jgre.20105](https://doi.org/10.1002/jgre.20105)
- Lillis, R. J., Deighan, J., Fox, J. L., et al. 2017, *Journal of Geophysical Research (Space Physics)*, 122, 3815, doi: [10.1002/2016JA023525](https://doi.org/10.1002/2016JA023525)
- Luger, R., & Barnes, R. 2015, *Astrobiology*, 15, 119, doi: [10.1089/ast.2014.1231](https://doi.org/10.1089/ast.2014.1231)
- Lustig-Yaeger, J., Fu, G., May, E. M., et al. 2023, *Nature Astronomy*, 7, 1317, doi: [10.1038/s41550-023-02064-z](https://doi.org/10.1038/s41550-023-02064-z)
- Mahaffy, P. R., Webster, C. R., Atreya, S. K., et al. 2013, *Science*, 341, 263, doi: [10.1126/science.1237966](https://doi.org/10.1126/science.1237966)
- Mangold, N. 2021, *Nature Geoscience*, 14, 112, doi: [10.1038/s41561-021-00700-9](https://doi.org/10.1038/s41561-021-00700-9)
- Mangold, N., Gupta, S., Gasnault, O., et al. 2021, *Science*, 374, 711, doi: [10.1126/science.abl4051](https://doi.org/10.1126/science.abl4051)
- Mao, S., & Paczynski, B. 1991, *ApJL*, 374, L37, doi: [10.1086/186066](https://doi.org/10.1086/186066)
- Marley, M. S., Gelino, C., Stephens, D., Lunine, J. I., & Freedman, R. 1999, *ApJ*, 513, 879, doi: [10.1086/306881](https://doi.org/10.1086/306881)
- Martin, R. G., & Livio, M. 2015, *ApJ*, 810, 105, doi: [10.1088/0004-637X/810/2/105](https://doi.org/10.1088/0004-637X/810/2/105)
- Matuszewski, F., Nettelmann, N., Cabrera, J., Börner, A., & Rauer, H. 2023, *A&A*, 677, A133, doi: [10.1051/0004-6361/202245287](https://doi.org/10.1051/0004-6361/202245287)
- McElroy, M. B. 1972, *Science*, 175, 443, doi: [10.1126/science.175.4020.443](https://doi.org/10.1126/science.175.4020.443)
- McElwain, M. W., Mawet, D., Ruffio, J.-B., et al. 2025, *arXiv e-prints*, arXiv:2510.02547, doi: [10.48550/arXiv.2510.02547](https://doi.org/10.48550/arXiv.2510.02547)
- Melosh, H. J., & Vickery, A. M. 1989, *Nature*, 338, 487, doi: [10.1038/338487a0](https://doi.org/10.1038/338487a0)
- Millan, M., Campbell, K. A., Sriaporn, C., et al. 2025, *Astrobiology*, 25, 225, doi: [10.1089/ast.2024.0020](https://doi.org/10.1089/ast.2024.0020)
- Milliken, R. E., Swayze, G. A., Arvidson, R. E., et al. 2008, *Geology*, 36, 847, doi: [10.1130/G24967A.1](https://doi.org/10.1130/G24967A.1)
- Millour, E., Forget, F., Spiga, A., et al. 2015, in *European Planetary Science Congress, EPSC2015–438*
- Millour, E., Forget, F., Spiga, A., et al. 2024, in *European Planetary Science Congress, EPSC2024–516*, doi: [10.5194/epsc2024-516](https://doi.org/10.5194/epsc2024-516)
- Mittelholz, A., Johnson, C. L., Feinberg, J. M., Langlais, B., & Phillips, R. J. 2020, *Science Advances*, 6, eaba0513, doi: [10.1126/sciadv.aba0513](https://doi.org/10.1126/sciadv.aba0513)
- Mogavero, F., & Laskar, J. 2021, *A&A*, 655, A1, doi: [10.1051/0004-6361/202141007](https://doi.org/10.1051/0004-6361/202141007)

- Morris, B. M., Bobra, M. G., Agol, E., Lee, Y. J., & Hawley, S. L. 2020, *MNRAS*, 493, 5489, doi: [10.1093/mnras/staa618](https://doi.org/10.1093/mnras/staa618)
- Muirhead, P. S., Johnson, J. A., Apps, K., et al. 2012, *ApJ*, 747, 144, doi: [10.1088/0004-637X/747/2/144](https://doi.org/10.1088/0004-637X/747/2/144)
- Mulders, G. D., Pascucci, I., Apai, D., & Ciesla, F. J. 2018, *AJ*, 156, 24, doi: [10.3847/1538-3881/aac5ea](https://doi.org/10.3847/1538-3881/aac5ea)
- Murray-Clay, R. A., Chiang, E. I., & Murray, N. 2009, *ApJ*, 693, 23, doi: [10.1088/0004-637X/693/1/23](https://doi.org/10.1088/0004-637X/693/1/23)
- Mustard, J. F., Murchie, S. L., Pelkey, S. M., et al. 2008, *Nature*, 454, 305, doi: [10.1038/nature07097](https://doi.org/10.1038/nature07097)
- Nair, H., Allen, M., Anbar, A. D., Yung, Y. L., & Clancy, R. T. 1994, *Icarus*, 111, 124, doi: [10.1006/icar.1994.1137](https://doi.org/10.1006/icar.1994.1137)
- Nielsen, E. L., De Rosa, R. J., Macintosh, B., et al. 2019, *AJ*, 158, 13, doi: [10.3847/1538-3881/ab16e9](https://doi.org/10.3847/1538-3881/ab16e9)
- Noack, L., Rivoldini, A., & Van Hoolst, T. 2017, *Physics of the Earth and Planetary Interiors*, 269, 40, doi: [10.1016/j.pepi.2017.05.010](https://doi.org/10.1016/j.pepi.2017.05.010)
- O'Brien, D. P., Walsh, K. J., Morbidelli, A., Raymond, S. N., & Mandell, A. M. 2014, *Icarus*, 239, 74, doi: [10.1016/j.icarus.2014.05.009](https://doi.org/10.1016/j.icarus.2014.05.009)
- O'Neill, C., & Lenardic, A. 2007, *Geophys. Res. Lett.*, 34, L19204, doi: [10.1029/2007GL030598](https://doi.org/10.1029/2007GL030598)
- Ostberg, C., Kane, S. R., Lincowski, A. P., & Dalba, P. A. 2023, *AJ*, 166, 213, doi: [10.3847/1538-3881/acfd2](https://doi.org/10.3847/1538-3881/acfd2)
- Owen, J. E. 2019, *Annual Review of Earth and Planetary Sciences*, 47, 67, doi: [10.1146/annurev-earth-053018-060246](https://doi.org/10.1146/annurev-earth-053018-060246)
- Paczynski, B. 1986, *ApJ*, 304, 1, doi: [10.1086/164140](https://doi.org/10.1086/164140)
- . 1996, *ARA&A*, 34, 419, doi: [10.1146/annurev.astro.34.1.419](https://doi.org/10.1146/annurev.astro.34.1.419)
- Pahlevan, K., & Stevenson, D. J. 2007, *Earth and Planetary Science Letters*, 262, 438, doi: [10.1016/j.epsl.2007.07.055](https://doi.org/10.1016/j.epsl.2007.07.055)
- Park, R. S., Folkner, W. M., Williams, J. G., & Boggs, D. H. 2021, *AJ*, 161, 105, doi: [10.3847/1538-3881/abd414](https://doi.org/10.3847/1538-3881/abd414)
- Paxton, B., Bildsten, L., Dotter, A., et al. 2011, *ApJS*, 192, 3, doi: [10.1088/0067-0049/192/1/3](https://doi.org/10.1088/0067-0049/192/1/3)
- Paxton, B., Cantiello, M., Arras, P., et al. 2013, *ApJS*, 208, 4, doi: [10.1088/0067-0049/208/1/4](https://doi.org/10.1088/0067-0049/208/1/4)
- Paxton, B., Marchant, P., Schwab, J., et al. 2015, *ApJS*, 220, 15, doi: [10.1088/0067-0049/220/1/15](https://doi.org/10.1088/0067-0049/220/1/15)
- Paxton, B., Schwab, J., Bauer, E. B., et al. 2018, *ApJS*, 234, 34, doi: [10.3847/1538-4365/aaa5a8](https://doi.org/10.3847/1538-4365/aaa5a8)
- Paxton, B., Smolec, R., Schwab, J., et al. 2019, *ApJS*, 243, 10, doi: [10.3847/1538-4365/ab2241](https://doi.org/10.3847/1538-4365/ab2241)
- Penny, M. T., Gaudi, B. S., Kerins, E., et al. 2019, *ApJS*, 241, 3, doi: [10.3847/1538-4365/aafb69](https://doi.org/10.3847/1538-4365/aafb69)
- Pepe, F., Cristiani, S., Rebolo, R., et al. 2021, *A&A*, 645, A96, doi: [10.1051/0004-6361/202038306](https://doi.org/10.1051/0004-6361/202038306)
- Pepin, R. O. 1991, *Icarus*, 92, 2, doi: [10.1016/0019-1035\(91\)90036-S](https://doi.org/10.1016/0019-1035(91)90036-S)
- Perryman, M., Hartman, J., Bakos, G. Á., & Lindegren, L. 2014, *ApJ*, 797, 14, doi: [10.1088/0004-637X/797/1/14](https://doi.org/10.1088/0004-637X/797/1/14)
- Piaulet-Ghorayeb, C., Benneke, B., Turbet, M., et al. 2025, *ApJ*, 989, 181, doi: [10.3847/1538-4357/adf207](https://doi.org/10.3847/1538-4357/adf207)
- Pollack, J. B., Kasting, J. F., Richardson, S. M., & Poliakoff, K. 1987, *Icarus*, 71, 203, doi: [10.1016/0019-1035\(87\)90147-3](https://doi.org/10.1016/0019-1035(87)90147-3)
- Quanz, S. P., Ottiger, M., Fontanet, E., et al. 2022, *A&A*, 664, A21, doi: [10.1051/0004-6361/202140366](https://doi.org/10.1051/0004-6361/202140366)
- Ramirez, R. M., & Kaltenegger, L. 2017, *ApJL*, 837, L4, doi: [10.3847/2041-8213/aa60c8](https://doi.org/10.3847/2041-8213/aa60c8)
- Rauer, H., Catala, C., Aerts, C., et al. 2014, *Experimental Astronomy*, 38, 249, doi: [10.1007/s10686-014-9383-4](https://doi.org/10.1007/s10686-014-9383-4)
- Rauer, H., Aerts, C., Cabrera, J., et al. 2025, *Experimental Astronomy*, 59, 26, doi: [10.1007/s10686-025-09985-9](https://doi.org/10.1007/s10686-025-09985-9)
- Raymond, S. N., & Izidoro, A. 2017, *Icarus*, 297, 134, doi: [10.1016/j.icarus.2017.06.030](https://doi.org/10.1016/j.icarus.2017.06.030)
- Raymond, S. N., Izidoro, A., & Morbidelli, A. 2020, in *Planetary Astrobiology*, ed. V. S. Meadows, G. N. Arney, B. E. Schmidt, & D. J. Des Marais (University of Arizona Press), 287, doi: [10.2458/azu_uapress.9780816540068](https://doi.org/10.2458/azu_uapress.9780816540068)
- Raymond, S. N., O'Brien, D. P., Morbidelli, A., & Kaib, N. A. 2009, *Icarus*, 203, 644, doi: [10.1016/j.icarus.2009.05.016](https://doi.org/10.1016/j.icarus.2009.05.016)
- Ricker, G. R., Winn, J. N., Vanderspek, R., et al. 2015, *Journal of Astronomical Telescopes, Instruments, and Systems*, 1, 014003, doi: [10.1117/1.JATIS.1.1.014003](https://doi.org/10.1117/1.JATIS.1.1.014003)
- Rigby, J., Perrin, M., McElwain, M., et al. 2023, *PASP*, 135, 048001, doi: [10.1088/1538-3873/acb293](https://doi.org/10.1088/1538-3873/acb293)
- Robinson, T. D., & Salvador, A. 2023, *PSJ*, 4, 10, doi: [10.3847/PSJ/acac9a](https://doi.org/10.3847/PSJ/acac9a)
- Rocchetti, G., Sterzik, M. F., Emde, C., et al. 2025a, *A&A*, 702, A262, doi: [10.1051/0004-6361/202555758](https://doi.org/10.1051/0004-6361/202555758)
- Rocchetti, G., Sterzik, M. F., Seidel, J. V., et al. 2025b, *A&A*, 700, A62, doi: [10.1051/0004-6361/202554831](https://doi.org/10.1051/0004-6361/202554831)
- Roettenbacher, R. M., & Kane, S. R. 2017, *ApJ*, 851, 77, doi: [10.3847/1538-4357/aa991e](https://doi.org/10.3847/1538-4357/aa991e)
- Rogers, L. A. 2015, *ApJ*, 801, 41, doi: [10.1088/0004-637X/801/1/41](https://doi.org/10.1088/0004-637X/801/1/41)
- Rousseau, H., Ertel, S., Defrère, D., Faramaz, V., & Wagner, K. 2024, *A&A*, 687, A147, doi: [10.1051/0004-6361/202348574](https://doi.org/10.1051/0004-6361/202348574)
- Saar, S. H., & Donahue, R. A. 1997, *ApJ*, 485, 319, doi: [10.1086/304392](https://doi.org/10.1086/304392)
- Saggese, V., Bachelet, É., Calchi Novati, S., et al. 2025, *arXiv e-prints*, arXiv:2512.05182, doi: [10.48550/arXiv.2512.05182](https://doi.org/10.48550/arXiv.2512.05182)

- Sajadian, S. 2021, *MNRAS*, 506, 3615, doi: [10.1093/mnras/stab1907](https://doi.org/10.1093/mnras/stab1907)
- Sako, T., Sekiguchi, T., Sasaki, M., et al. 2008, *Experimental Astronomy*, 22, 51, doi: [10.1007/s10686-007-9082-5](https://doi.org/10.1007/s10686-007-9082-5)
- Schneider, J., Dedieu, C., Le Sidaner, P., Savalle, R., & Zolotukhin, I. 2011, *A&A*, 532, A79, doi: [10.1051/0004-6361/201116713](https://doi.org/10.1051/0004-6361/201116713)
- Schwab, C., Rakich, A., Gong, Q., et al. 2016, in *Society of Photo-Optical Instrumentation Engineers (SPIE) Conference Series*, Vol. 9908, *Ground-based and Airborne Instrumentation for Astronomy VI*, ed. C. J. Evans, L. Simard, & H. Takami, 99087H, doi: [10.1117/12.2234411](https://doi.org/10.1117/12.2234411)
- Schwieterman, E. W., Kiang, N. Y., Parenteau, M. N., et al. 2018, *Astrobiology*, 18, 663, doi: [10.1089/ast.2017.1729](https://doi.org/10.1089/ast.2017.1729)
- Seifahrt, A., Bean, J. L., Stürmer, J., et al. 2016, in *Society of Photo-Optical Instrumentation Engineers (SPIE) Conference Series*, Vol. 9908, *Ground-based and Airborne Instrumentation for Astronomy VI*, ed. C. J. Evans, L. Simard, & H. Takami, 990818, doi: [10.1117/12.2232069](https://doi.org/10.1117/12.2232069)
- Shields, A. L., Ballard, S., & Johnson, J. A. 2016, *PhR*, 663, 1, doi: [10.1016/j.physrep.2016.10.003](https://doi.org/10.1016/j.physrep.2016.10.003)
- Shoji, D., & Kurita, K. 2014, *ApJ*, 789, 3, doi: [10.1088/0004-637X/789/1/3](https://doi.org/10.1088/0004-637X/789/1/3)
- Stark, C. C., Latouf, N., Mandell, A. M., & Young, A. 2024a, *Journal of Astronomical Telescopes, Instruments, and Systems*, 10, 014005, doi: [10.1117/1.JATIS.10.1.014005](https://doi.org/10.1117/1.JATIS.10.1.014005)
- Stark, C. C., Mennesson, B., Bryson, S., et al. 2024b, *Journal of Astronomical Telescopes, Instruments, and Systems*, 10, 034006, doi: [10.1117/1.JATIS.10.3.034006](https://doi.org/10.1117/1.JATIS.10.3.034006)
- Stassun, K. G., Collins, K. A., & Gaudi, B. S. 2017, *AJ*, 153, 136, doi: [10.3847/1538-3881/aa5df3](https://doi.org/10.3847/1538-3881/aa5df3)
- Sudarsky, D., Burrows, A., & Pinto, P. 2000, *ApJ*, 538, 885, doi: [10.1086/309160](https://doi.org/10.1086/309160)
- Sun, V. Z., & Milliken, R. E. 2018, *Geophys. Res. Lett.*, 45, 10,221, doi: [10.1029/2018GL078494](https://doi.org/10.1029/2018GL078494)
- Tasker, E., Tan, J., Heng, K., et al. 2017, *Nature Astronomy*, 1, 0042, doi: [10.1038/s41550-017-0042](https://doi.org/10.1038/s41550-017-0042)
- Terry, S. K., Bachelet, E., Zohrabi, F., et al. 2025, *arXiv e-prints*, arXiv:2510.13974, doi: [10.48550/arXiv.2510.13974](https://doi.org/10.48550/arXiv.2510.13974)
- The LUVVOIR Team. 2019, *arXiv e-prints*, arXiv:1912.06219. <https://arxiv.org/abs/1912.06219>
- Tian, F. 2009, *ApJ*, 703, 905, doi: [10.1088/0004-637X/703/1/905](https://doi.org/10.1088/0004-637X/703/1/905)
- Tian, F., Kasting, J. F., & Solomon, S. C. 2009, *Geophys. Res. Lett.*, 36, L02205, doi: [10.1029/2008GL036513](https://doi.org/10.1029/2008GL036513)
- Tinetti, G., Meadows, V. S., Crisp, D., et al. 2005, *Astrobiology*, 5, 461, doi: [10.1089/ast.2005.5.461](https://doi.org/10.1089/ast.2005.5.461)
- Tosi, N., Godolt, M., Stracke, B., et al. 2017, *A&A*, 605, A71, doi: [10.1051/0004-6361/201730728](https://doi.org/10.1051/0004-6361/201730728)
- Touma, J., & Wisdom, J. 1993, *Science*, 259, 1294, doi: [10.1126/science.259.5099.1294](https://doi.org/10.1126/science.259.5099.1294)
- Tuchow, N. W., Stark, C. C., & Mamajek, E. 2024, *AJ*, 167, 139, doi: [10.3847/1538-3881/ad25ec](https://doi.org/10.3847/1538-3881/ad25ec)
- Turbet, M., Leconte, J., Selsis, F., et al. 2016, *A&A*, 596, A112, doi: [10.1051/0004-6361/201629577](https://doi.org/10.1051/0004-6361/201629577)
- Turbet, M., Bolmont, E., Leconte, J., et al. 2018, *A&A*, 612, A86, doi: [10.1051/0004-6361/201731620](https://doi.org/10.1051/0004-6361/201731620)
- Udalski, A., Szymański, M. K., & Szymański, G. 2015, *AcA*, 65, 1, doi: [10.48550/arXiv.1504.05966](https://doi.org/10.48550/arXiv.1504.05966)
- Unterborn, C. T., Desch, S. J., Haldemann, J., et al. 2023, *ApJ*, 944, 42, doi: [10.3847/1538-4357/aca3b](https://doi.org/10.3847/1538-4357/aca3b)
- Unterborn, C. T., Foley, B. J., Desch, S. J., et al. 2022, *ApJL*, 930, L6, doi: [10.3847/2041-8213/ac6596](https://doi.org/10.3847/2041-8213/ac6596)
- Van Laerhoven, C., Barnes, R., & Greenberg, R. 2014, *MNRAS*, 441, 1888, doi: [10.1093/mnras/stu685](https://doi.org/10.1093/mnras/stu685)
- Vanderburg, A., Plavchan, P., Johnson, J. A., et al. 2016, *MNRAS*, 459, 3565, doi: [10.1093/mnras/stw863](https://doi.org/10.1093/mnras/stw863)
- Villanueva, G. L., Smith, M. D., Protopapa, S., Faggi, S., & Mandell, A. M. 2018, *JQSRT*, 217, 86, doi: [10.1016/j.jqsrt.2018.05.023](https://doi.org/10.1016/j.jqsrt.2018.05.023)
- Voigt, J. R. C., Sun, V. Z., Viviano, C. E., & Stack, K. M. 2024, *Geophys. Res. Lett.*, 51, e2024GL108610, doi: [10.1029/2024GL108610](https://doi.org/10.1029/2024GL108610)
- Walsh, K. J., Morbidelli, A., Raymond, S. N., O'Brien, D. P., & Mandell, A. M. 2011, *Nature*, 475, 206, doi: [10.1038/nature10201](https://doi.org/10.1038/nature10201)
- Ward, W. R. 1973, *Science*, 181, 260, doi: [10.1126/science.181.4096.260](https://doi.org/10.1126/science.181.4096.260)
- Warren, A. O., Kite, E. S., Williams, J.-P., & Horgan, B. 2019, *Journal of Geophysical Research (Planets)*, 124, 2793, doi: [10.1029/2019JE006178](https://doi.org/10.1029/2019JE006178)
- Way, M. J., & Georgakarakos, N. 2017, *ApJ*, 835, L1, doi: [10.3847/2041-8213/835/1/L1](https://doi.org/10.3847/2041-8213/835/1/L1)
- Webster, C. R., Mahaffy, P. R., Flesch, G. J., et al. 2013, *Science*, 341, 260, doi: [10.1126/science.1237961](https://doi.org/10.1126/science.1237961)
- Westall, F., Foucher, F., Bost, N., et al. 2015, *Astrobiology*, 15, 998, doi: [10.1089/ast.2015.1374](https://doi.org/10.1089/ast.2015.1374)
- Winn, J. N., & Fabrycky, D. C. 2015, *ARA&A*, 53, 409, doi: [10.1146/annurev-astro-082214-122246](https://doi.org/10.1146/annurev-astro-082214-122246)
- Wolfe, C. A., & Robinson, T. D. 2024, *Planet. Space Sci.*, 250, 105944, doi: [10.1016/j.pss.2024.105944](https://doi.org/10.1016/j.pss.2024.105944)
- Wordsworth, R. 2015, *ApJ*, 806, 180, doi: [10.1088/0004-637X/806/2/180](https://doi.org/10.1088/0004-637X/806/2/180)

- Wordsworth, R. D. 2016, *Annual Review of Earth and Planetary Sciences*, 44, 381, doi: [10.1146/annurev-earth-060115-012355](https://doi.org/10.1146/annurev-earth-060115-012355)
- Wray, J. J., & Ehlmann, B. L. 2011, *Planet. Space Sci.*, 59, 196, doi: [10.1016/j.pss.2010.05.006](https://doi.org/10.1016/j.pss.2010.05.006)
- Wunderlich, F., Godolt, M., Grenfell, J. L., et al. 2019, *A&A*, 624, A49, doi: [10.1051/0004-6361/201834504](https://doi.org/10.1051/0004-6361/201834504)
- Zahnle, K., Haberle, R. M., Catling, D. C., & Kasting, J. F. 2008, *Journal of Geophysical Research (Planets)*, 113, E11004, doi: [10.1029/2008JE003160](https://doi.org/10.1029/2008JE003160)
- Zang, W., Han, C., Kondo, I., et al. 2021, *Research in Astronomy and Astrophysics*, 21, 239, doi: [10.1088/1674-4527/21/9/239](https://doi.org/10.1088/1674-4527/21/9/239)
- Zang, W., Jung, Y. K., Yee, J. C., et al. 2025, *Science*, 388, 400, doi: [10.1126/science.adn6088](https://doi.org/10.1126/science.adn6088)
- Zeebe, R. E. 2015, *ApJ*, 798, 8, doi: [10.1088/0004-637X/798/1/8](https://doi.org/10.1088/0004-637X/798/1/8)
- Zhang, M., Hu, R., Inglis, J., et al. 2024, *ApJL*, 961, L44, doi: [10.3847/2041-8213/ad1a07](https://doi.org/10.3847/2041-8213/ad1a07)
- Zieba, S., Kreidberg, L., Ducrot, E., et al. 2023, *Nature*, 620, 746, doi: [10.1038/s41586-023-06232-z](https://doi.org/10.1038/s41586-023-06232-z)